

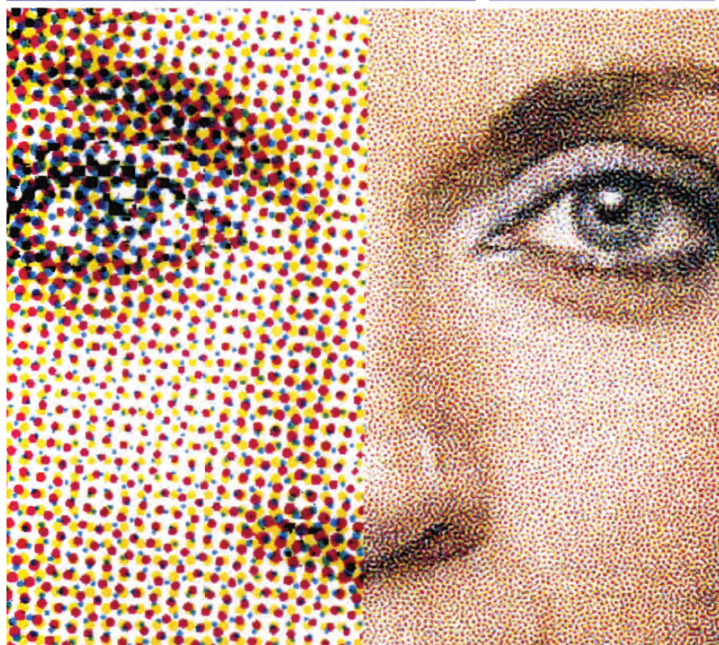


University of Novi Sad
Faculty of Technical Sciences
DEPARTMENT OF GRAPHIC
ENGINEERING AND DESIGN

Volume **12**
Number **2**
June **2021**

JGED

JOURNAL OF GRAPHIC
ENGINEERING AND DESIGN



Aiming for G7 Master Compliance through a Color Managed Workflow: Comparison of Compliance with Amplitude Modulated (AM) vs. Frequency Modulated (FM) Screening of Multicolor Digital Printing

Haji Naik Dharavath

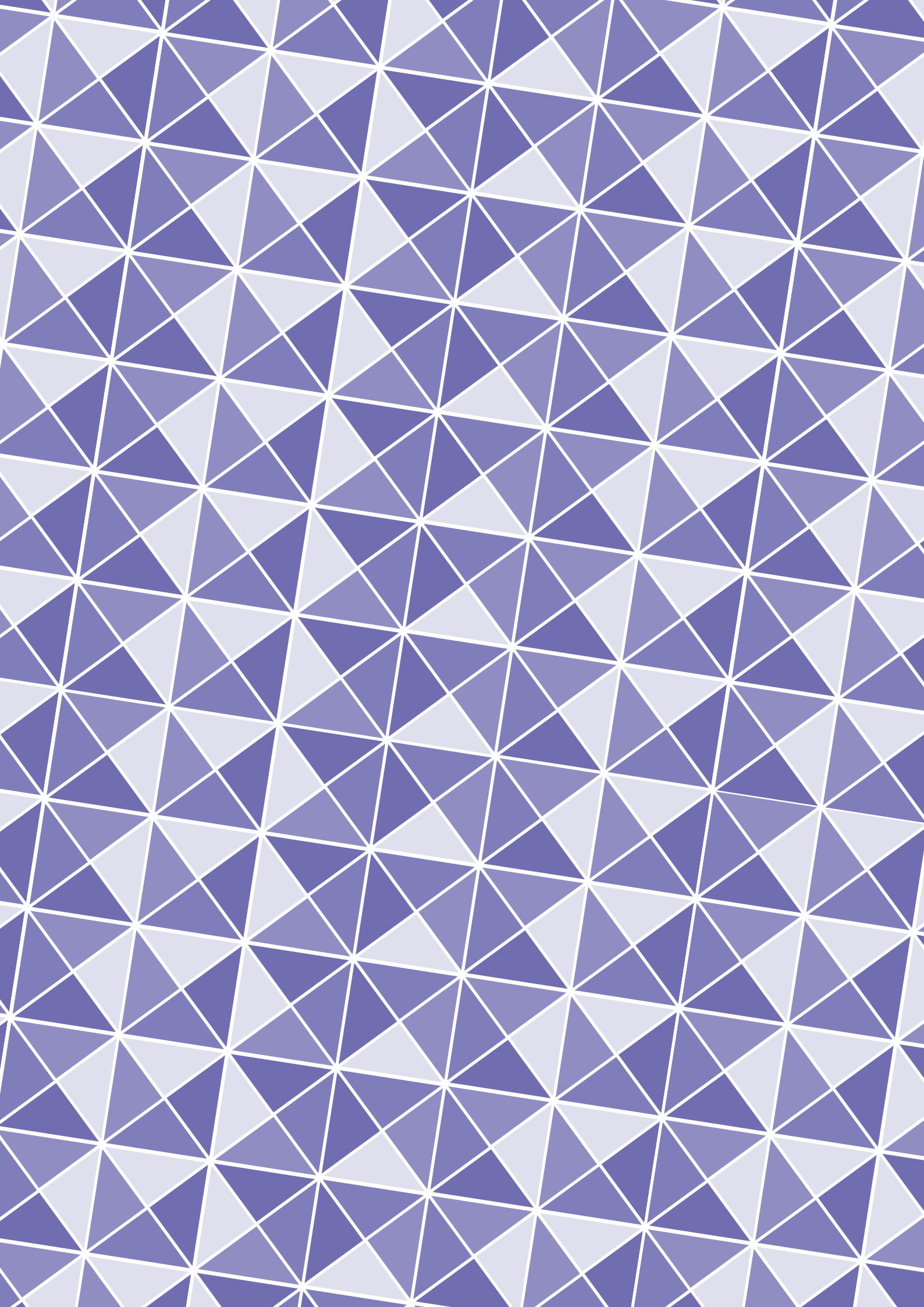
The effect of electromagnetic radiation on the reflectance spectra of prints on hemp papers

Ivana Plazonić, Vesna Džimbeg-Malčić,
Irena Bates, Gabriel Žilić



Drying methods of the printing inks
Ashraf Abd El-Rahman, Elsayed Saad,
Cem Aydemir, Samed Ayhan Özsoy,
Semiha Yenidoğan

Impact of packaging shape and material on consumer expectations
Suzana Poslon, Dorotea Kovačević, Maja Brozović



JGED

JOURNAL OF GRAPHIC
ENGINEERING AND DESIGN

2/2021

Volume 12, Number 2, June 2021.

Published by

UNIVERSITY OF NOVI SAD, SERBIA
Faculty of Technical Sciences
Department of Graphic Engineering and Design

PUBLISHED BY



University of Novi Sad
Faculty of Technical Sciences

DEPARTMENT OF GRAPHIC
ENGINEERING AND DESIGN

Address:

Faculty of Technical Sciences,
Department of Graphic
Engineering and Design,

Trg Dositeja Obradovića 6
21000 Novi Sad, Serbia

Telephone numbers:

+381 21 485 26 20
+381 21 485 26 26
+381 21 485 26 21

Fax number:

+381 21 485 25 45

Email:

jged@uns.ac.rs

Web address:

www.grid.uns.ac.rs/jged

Frequency: 4 issues per year

Printing: Faculty of Technical Sciences,
Department of Graphic Engineering and Design

Circulation: 200

Electronic version of journal available on
www.grid.uns.ac.rs/jged

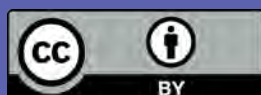
E-ISSN 2217-9860

The journal is abstracted/indexed
in the Scopus and Directory of Open Access Journals



CIP - Katalogizacija u publikaciji
Biblioteka Matice srpske, Novi Sad
655

JGED : Journal of Graphic Engineering and Design /
editor Dragoljub Novaković. - Vol. 1, No. 1 (nov. 2010) -
Sciences, Department of Graphic Engineering and
Design,
2010-. 30 cm
Četiri puta godišnje
ISSN 2217-379X
COBISS.SR-ID 257662727



© 2021 Authors. Published by the University of Novi Sad, Faculty of
Technical Sciences, Department of Graphic Engineering and Design. All
articles are an open access articles distributed under the terms and con-
ditions of the Creative Commons Attribution license 3.0 Serbia (<http://creativecommons.org/licenses/by/3.0/rs/>).

EDITORS

Dragoljub Novaković, University of Novi Sad, Novi Sad, Serbia

Nemanja Kašiković, University of Novi Sad, Novi Sad, Serbia

EDITORIAL BOARD

Thomas Hoffmann-Walbeck

HDM Stuttgart, Stuttgart, Germany

Rafael Huertas

University of Granada, Granada, Spain

Joanna Ewa Izdebska

Warsaw University of Technology, Warsaw, Poland

Igor Majnarić

University of Zagreb, Zagreb, Croatia

Branko Milosavljević

University of Novi Sad, Novi Sad, Serbia

Deja Muck

University of Ljubljana, Ljubljana, Slovenia

László Koltai

Óbuda University, Budapest, Hungary

Anastasios E. Politis

Hellenic Union of Graphic Arts and Media Technology Engineers-
HELGRAMED, Athens, Greece

Miljana Prica

University of Novi Sad, Novi Sad, Serbia

Iskren Spiridonov

University of Chemical Technology and Metallurgy,
Sofia, Bulgaria

Mladen Stančić

University of Banja Luka, Banja Luka, Bosnia and Herzegovina

Tomáš Syrový

University of Pardubice, Pardubice, Czech Republic

Gojko Vladić

University of Novi Sad, Novi Sad, Serbia

Thomas Sabu

Mahatma Gandhi University, Kottayam, India

Jonas Malinauskas

Vilnius College of Technologies and Design, Vilnius, Lithuania

Roberto Pašić

UKLO University St. Climent Ohridski, Bitola, North Macedonia

Behudin Mešić

SCION, Rotorua, New Zealand

Arif Özcan

Marmara University, Istanbul, Turkey

Vladan Končar

ENSAIT, Roubaix, France

Catarina Silva

Polytechnic Institute of Cávado and Ave (IPCA), Barcelos, Portugal

Michal Čeppan

Slovak University of Technology in Bratislava, Slovakia

Tim C Claypole

Swansea University, Swansea, United Kingdom

Alexandra Pekarovicova

Western Michigan University, Kalamazoo, USA

Panagiotis Kyratsis

University of Western Macedonia, Kozani, Greece

Jason Lisi

Ryerson University, Toronto, Canada

Peter Nussbaum

Norwegian University of Science and Technology, Gjøvik, Norway

Art Director

Uroš Nedeljković

Layout design

Bojan Banjanin

Journal cover design

Nada Miketić

Contents

- 5 **Aiming for G7 Master Compliance through a Color Managed Workflow: Comparison of Compliance with Amplitude Modulated (AM) vs. Frequency Modulated (FM) Screening of Multicolor Digital Printing**
Haji Naik Dharavath
- 21 **The effect of electromagnetic radiation on the reflectance spectra of prints on hemp papers**
*Ivana Plazonić, Vesna Džimbeg-Malčić,
Irena Bates, Gabriel Žilić*
- 29 **Drying methods of the printing inks**
*Ashraf Abd El-Rahman Elsayed Saad, Cem Aydemir,
Samed Ayhan Özsoy, Semiha Yenidoğan*
- 39 **Impact of packaging shape and material on consumer expectations**
Suzana Poslon, Dorotea Kovačević, Maja Brozović


Aiming for G7 Master Compliance through a Color Managed Workflow: Comparison of Compliance with Amplitude Modulated (AM) vs. Frequency Modulated (FM) Screening of Multicolor Digital Printing

ABSTRACT

The purpose of this research was to determine the influence of screening technologies (AM vs. FM) in the color reproduction aimed at the G7 master compliance. The quality of digital color printing is determined by these influential factors: screening method applied, type of printing process, ink (dry-toner or liquid-toner), printer resolution and the substrate (paper). For this research, only the color printing attributes such as the G7 colors hue and chroma, gray balance, and overall color deviations were analyzed to examine the significant differences that exist between the two screening technologies (AM vs. FM). These are the color attributes which are monitored and managed for quality accuracy during the printing. Printed colorimetry of each screening from the experiment was compared against G7 ColorSpace GRACoL 2013 (CGATS21-2-CRPC6) in CIE L a* b* space using an IDEAlliance (Chromix/Hutch Color) Curve 4.2.4 application interface with an X-Rite spectrophotometer with an i1iO table. The measured data of each screening were run through this application (Curve 4.2.4). The data of each screening were analyzed by using the Verify Tool of the Curve 4.2.4 application to determine the pass/fail of G7 master compliance levels using G7 ColorSpace tolerances (G7 Grayscale, G7 Targeted, and G7 Colorspace). Analyzed data from the experiment revealed that the printed colorimetric values of each screening (G7 Grayscale, G7 Targeted, and G7 Colorspace) are in match (aligned) with the G7 master compliance levels (reference/target) colorimetric values (G7 Grayscale, G7 Targeted, and G7 Colorspace). Therefore, the press run was passed by the Curve 4 application for both screening technologies tested.*

KEY WORDS

G7, calibration, color, colorimetry, gamut, profiling, screening

Haji Naik Dharavath 

Central Connecticut State University, Department of Computer Electronics & Graphics Technology, New Britain, USA

Corresponding author:
Haji Naik Dharavath
e-mail: dharavathh@ccsu.edu

First received: 15.12.2020.

Revised: 9.2.2021.

Accepted: 25.2.2021.

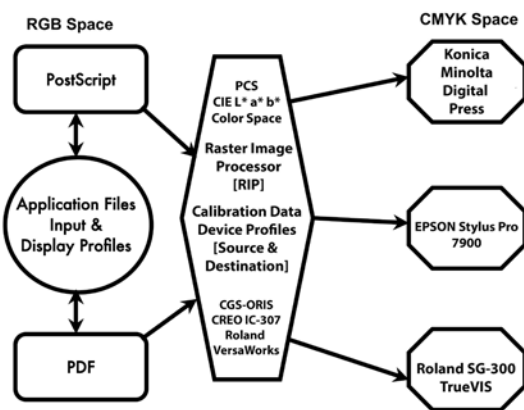
Introduction

A continuous-tone color image is composed of a full spectrum of shades and color, from near white to dense black. In a traditional printing (offset, digital offset, gravure or flexography) workflow, the method by which continuous-tone photographic images are transformed

to a printable image is called halftoning. In this method, varying percentages of the printed sheet are covered with halftone dots to represent the varying tones in the image. The ink (paste or liquid ink or dry toner) printed by each dot, of course, has the same density. At normal viewing distance, the dots of a printed image create an optical illusion of a continuous tone image. In contrast, a

simple digital image could be a binary picture, $[h(x, y)]$, with each point being either completely black or completely white (Pnueli & Bruckstein, 1996). A digital halftone is a pixel map, with bit depth, that gives the impression of an image containing a range of gray shades or continuous tones. An 8-bit grayscale image contains 256 different levels of gray from white to black.

A modern and up-to-date commercial printing workflow requires a Color Management System (CMS) to produce a quality color printing. A CMS enables the color producer (printer operator or the designer) to deliver accurate output colors regardless of device color capacities with the use of proper color management techniques (see Figure 1). Analyzing the color image by examining its quantitative attributes eliminates the subjective judgment of color quality evaluation of printed colors or colors in nature. Advancements in science and engineering, however, have allowed print and graphic professionals to apply scientific research methods across printing workflow. Applying these methods heightens the importance of proper print production workflow.



» **Figure 1:** Schematics of Color Management System (CMS)

Rationale for literature review

Workflow is represented through schematic illustrations of activities that reflect the systematic organization of analog and digital devices used during the print and image production process. A print ready e-file (.PDF or .JPEG or .PSD or PostScript, etc.) is likely to be manipulated and later printed by an array of output digital devices [computer-to-plate (CTP), digital printers and printing presses]. Given each family of devices tends to create and produce color differently, the challenge is to manage color consistency across the entire workflow. Digital color print reproduction involves physical/mechanical interaction among the imaging cylinder, dry/liquid toner, and the substrate (Novaković & Avramović, 2012). The outcome of this interaction is the color print. Color can

be viewed as a science where the optical aspects of color are quantitatively analyzable and measurable. The human eye, however, perceives color more subjectively, which poses a challenge at times for the printing and image reproduction industry.

G7 stands for grayscale (or gray) plus the seven primary and secondary colors known as the subtractive and additive: Cyan, Magenta, Yellow, Black (CMYK) and Red, Green, Blue (RGB). G7 is a method which specifies calibration procedures for printing visually acceptable colors with an emphasis on matching colorimetrically derived aim-points for the print reproduction processes to print with a common visual appearance. Today, this method (G7) is used in many applications of printing such as offset lithography, flexography, and digital (color laser or inkjet). It uses a pre-defined one-dimensional neutral print density curve (NPDC) to match neutral tonality/gray balance. G7 specifications are owned by International Digital Enterprise Alliance (International Digital Enterprise Alliance- IDEAlliance, 2014) and the colorimetric formulas of the G7 are defined in the American National Standards Institute and the Committee on Graphic Arts Technology Standards/Technical Report (ANSI/CGATS TR015). Published reports reveal there are three ways G7 master compliance can be achieved: a) output device NPDC to G7 NPDC [P2P251x target image], b) use of output device ICC profile, and c) the use of device link profile (DLP = source as GRACoL2013 ICC profile + the destination device ICC profile). G7 master compliance includes three levels in the G7 master qualification: G7 Grayscale, G7 Targeted, and G7 Colorspace. These levels demonstrate G7 master capabilities of a print facility.

G7 Grayscale

This is the fundamental level of G7 commonly seen in most color print reproduction. Regardless of printing process, if a digital printer or printing press reproduces the defined neutral tone ramp as a neutral gray, then all other colors in the reproduction are believed to be without colorcast. This is determined by printing a target specified on a stable printing system and then measuring the target using the correct ink/toner curves to bring the printing system into alignment with the G7 ideal neutral density curve. Aligning the various reproduction processes and obtaining the same neutral aim points is critical for consistent reproduction.

G7 Targeted

The secondary level of G7 is achieved when G7 grayscale is matched and the solid ink measurements for primary and secondary (CMY and RGB) are also within the G7 target specifications. This can be achieved through the absolute white point or using the substrate-relative conditions. However, G7 Targeted compliance is not limited to the reference print conditions in ISO 12647-2 or in ISO/

PAS 15339. The G7-calibrated dataset can be used as a G7 reference print condition. G7 Targeted achievement certifies that the facility not only conforms to G7 Grayscale, but it can also achieve a higher level of compliance.

G7 Colorspace

The highest level of G7 compliance and the most stringent is the G7 Colorspace. It includes all the requirements of the G7 Targeted level and, therefore, the G7 Grayscale level. This also includes the matching of an entire Reference Print Condition (RPC). This level of control demonstrates that the reproduction maintains an extremely tight tolerance throughout the complete color space. An entire TC1617x target is printed and compared against the specific color space with all 1617 patches held to within a tight tolerance. This assures the printing system will reproduce the entire color space, not just the primary and secondary colors of CMYK and RGB. The G7 Colorspace can also relate to either the absolute white point or the substrate-relative aim values.

Regardless what experts (published reports) say, there is no single/fixed screening method that would work for every color reproduction. Since the introduction of digital workflow (computer to film, to plate, and to press) in the industry, there are many experts who have come up with technologies and tools for color images that would benefit from improved color reproduction technologies. Screening is only an option of such technologies. In the digital printing environment, screening software can create the digital version of the amplitude modulate (AM) and also of the frequency modulated (FM) halftone screen. Screening software in the raster image processor (RIP) of the color managed workflow (CMW) at a digital printing press front-end platform (DFE) applies a digital dot pattern to the color image during printing.

Gray balance represents the combination of specific amounts of cyan, magenta, and yellow inks to produce a neutral shade of gray. With slight increases in cyan pigment required to produce a neutral gray, shifts in hue will occur with any imbalance of these three components. In addition to the color gamut, the gray balance is an additional requirement for pleasing color-reproduction. In large part, the imbalance is due to impurities of the inks, chromaticity deviation of the substrates, or other attributes. To establish the proper gray balance for a specific process, a full set of tint charts can be reproduced. Careful evaluation of the printed tint charts will provide the specific values for that specific reproduction process. The ISO 12647-7 document states that the gray balance can be printed and measured at the CMY overlap (overlap of C = 50%, M = 40%, and Y = 40%). The deviation can be determined from the calculation of ΔH^* (deviation of hue, h^*) or ΔC^* (deviation of chroma, c^*) and it requires the colorimetric data of CMY overlap printing from the $L^* a^* b^*$ model.

The quality of a color image reproduced through any printing process (digital or traditional) is largely influenced by the properties of paper. While paper is considered a commodity, its properties are a long way from being standardized (Wales, 2009). Additional attributes must be monitored in order to produce quality printed materials. The press operator must carefully manage several print parameters, such as the source colors (a source profile of ISO or ANSI standard), press calibration, press characterization (device destination profile), and the screening option. Without controlling these parameters to a print job a color mismatch would result.

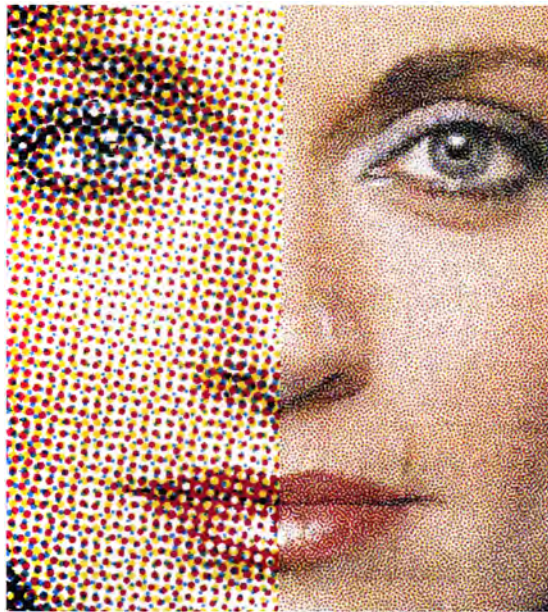
Amplitude Modulated (AM) Screening

In AM screening, the dot frequency is constant and dot amplitude varies. AM screening breaks the image into dots of varying sizes, which are clustered together, at a fixed screen angle. For each color (CMYK) to be overprinted, the halftone CMYK separations need to be generated at a particular screen angle to avoid a moiré pattern. The dot is generated from a cluster of laser spots. A halftone cell (or grid) is then divided into a matrix of single recording dots (laser spots). Since there is always a physical and mathematical relationship among the number of gray levels, the resolution of the output device, and the screen ruling, there is always a tradeoff between resolution and the number of reproducible gray levels (Fleming, Dollak & Fryzlewicz, 2004). The number of laser spots within a halftone cell depends on the following parameters: screen frequencies/screen angles, imagesetter resolution/gray levels, dot size, and dot shape/dot patterns. The outcome of the clustering is a continuous tone pattern – lighter or darker shades or tones (See Figure 2).

Frequency Modulated (FM) Screening

In FM screening, the dot frequency varies, and dot size is constant (Ma, 2003). FM screening, also referred to as stochastic screening, can be regarded as an electronic implementation of screenless printing (Chung & Ma, 1995). The word stochastic means “involving a random variable” – it uses randomly placed dots instead of AM halftone dots aligned along the screen angle. FM screening uses a microdot placement (See Figure 2). The dot size is fixed, but the number of dots within a halftone cell varies according to the tonal value being imaged. The minimum size of the dots is limited only by the output device resolution and dots are measured in microns (μm). A typical modern 2400 DPI output device has a laser spot size of 10.6 μm (microns, 10^{-6}) and the size of a microdot is 21 μm (Chung & Ma, 1995). In FM screening, screen angles are not required when generating a CMYK separation. This results in the eradication of the moiré pattern in the printed image (Fleming, Dollak & Fryzlewicz, 2004). FM screening, though, uses smaller dots that are not

restricted to a fixed grid pattern. By varying the number of dots in a given area, any desired gray level can be generated. The dots are smaller than the AM screening, therefore FM screening can represent more detail and support higher resolution printing (See Figure 2).



» **Figure 2:** AM (left) vs FM (right) Screened image
(Source: Creo Review)

Purpose of the research

The purpose of this applied research was to demonstrate the use of a complete color managed workflow (CMW) and meet the specified G7 master compliance levels by creating and using output device ICC profiles. The experiment was conducted in a color managed digital color printing workflow (CMDPW) to determine the **effect that screening technologies** have on the G7 master compliance: *Comparison of Compliance with Amplitude Modulated (AM) vs. Frequency Modulated (FM) Screening of Multicolor Digital Printing*. It was aimed at achieving the G7 master compliance through an ICC based CMW. As stated earlier, the G7 master compliance print evaluation can be achieved by use of the output device ICC profile for printing. This experiment adopts this method to achieve the compliance. G7 master compliance includes three compliance levels in the G7 master qualification: G7 Grayscale, G7 Targeted, and G7 Colorspace. These levels demonstrate G7 master capabilities of a print facility. *The G7 calibration method, using the P2P251x target was NOT considered to derive the device NPDC to compare with G7 NPDC for print (or press) runs 1, 2, 3, etc.*

Limitations of the Research

For this experiment, there were limitations to the technology used within the graphics program laboratory. Prior to printing and measuring the samples, the digital color output printing device and color measuring instruments (spectrophotometer and densitometer) were calibrated against the recommended reference. The print condition associated with this experiment was characterized by, but not restricted to, inherent limitations: colored images (TC1617x, ISO300, and ISO12647-7) chosen for printing, desired rendering intent applied, type of digital printer for proofing/printing, type of paper for printing, type of toner, resolution, screening technique, use of defined color output profiles, calibration data applied, and so on. Several variables affected the facsimile reproduction of color images in the CMDPW and most of them were mutually dependent. The scope of the research was limited to the color laser (electrophotographic) digital printing system (printing proof/printing) and other raw materials and the multiple types of color measuring devices and color management and control applications (data collection, data analysis, profile creation, and profile inspection) used at the university graphics laboratory. Findings were not expected to be generalizable to other CMDPW environments. It is quite likely, however, that others could find the method used and the data of this article meaningful and useful. The research methodology, experimental design, and statistical analysis were selected to align with the purpose of the research, taking into account the aforementioned limitations.

Research methodology

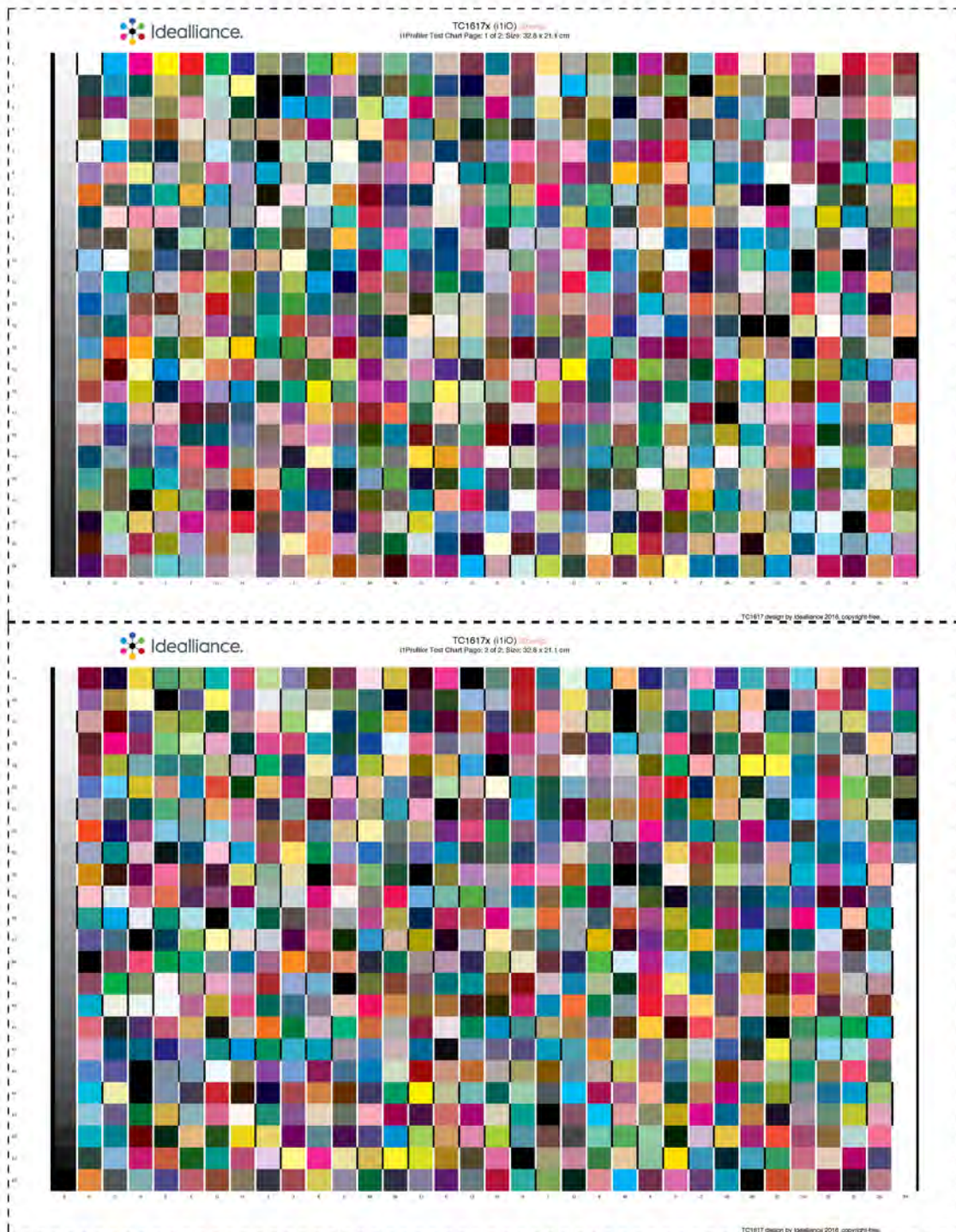
The digital color printing device used in this experiment is a Konica-Minolta bizHub C6000 Digital Color Press. It uses a Creo IC-307 raster image process (RIP) application (front-end system). A two-page custom test image (12" x 18" size) was created for proofing and printing use for the experiment (See Figures 3 & 3A). The test target contained the following elements: an ISO 300 and generic images for subjective evaluation of color, an ISO 12647-7 Control Strips (2013, three-tier), and a TC1617x target for gamut/profile creation. Colorimetric, Densitometric, and Spectrophotometric data were extracted by using an X-Rite Eye-One Spectrophotometer and an X-Rite i1i0 Scanning Spectrophotometer from the color printed samples for the analysis. For both screening technologies ($K = 2$), a total of 200 samples of target color images were printed, 100 prints for each screening method, noted by letter "N" ($N = 100$). Of 100 samples of each group, 80 samples ($n = 80$) were randomly selected from each screening group, and measured, noted by the letter "n" ($n = 80$).

Aiming for G7 Master Compliance through a Color Managed Workflow: Comparison of Compliance with Amplitude Modulated (AM) vs. Frequency Modulated (FM) Screening of Multicolor Digital Printing



» Figure 3: Test Image for the experiment (PAGE 01)

Aiming for G7 Master Compliance through a Color Managed Workflow: Comparison of Compliance with Amplitude Modulated (AM) vs. Frequency Modulated (FM) Screening of Multicolor Digital Printing



» **Figure 3A:** Test Image for the experiment (PAGE 02)

This sample size is needed to make the reliability of data is accurate. It is well documented that a large sample size is more representative of the sampling population (subjects). Each printed sheet is measured by using the scan-

ning spectrophotometer, data was then saved, and later combined in the Chromix/IDEAlliance Curve 4 application for the analysis. Glass, G.V. & Hopkins, K.D. (1996) provides an objective method to determine the sample size

when the size of the total population is known. The following formula was used to determine the required sample size, which was 80 (n) printed sheets for this study:

$$n = \frac{[\chi^2 NP (1-P)]}{[d^2 (N-1) + \chi^2 P (1-P)]} \quad (1)$$

n = the required sample size

χ^2 = the table value of chi-square for 1 degree of freedom at the desired confidence level (3.84)

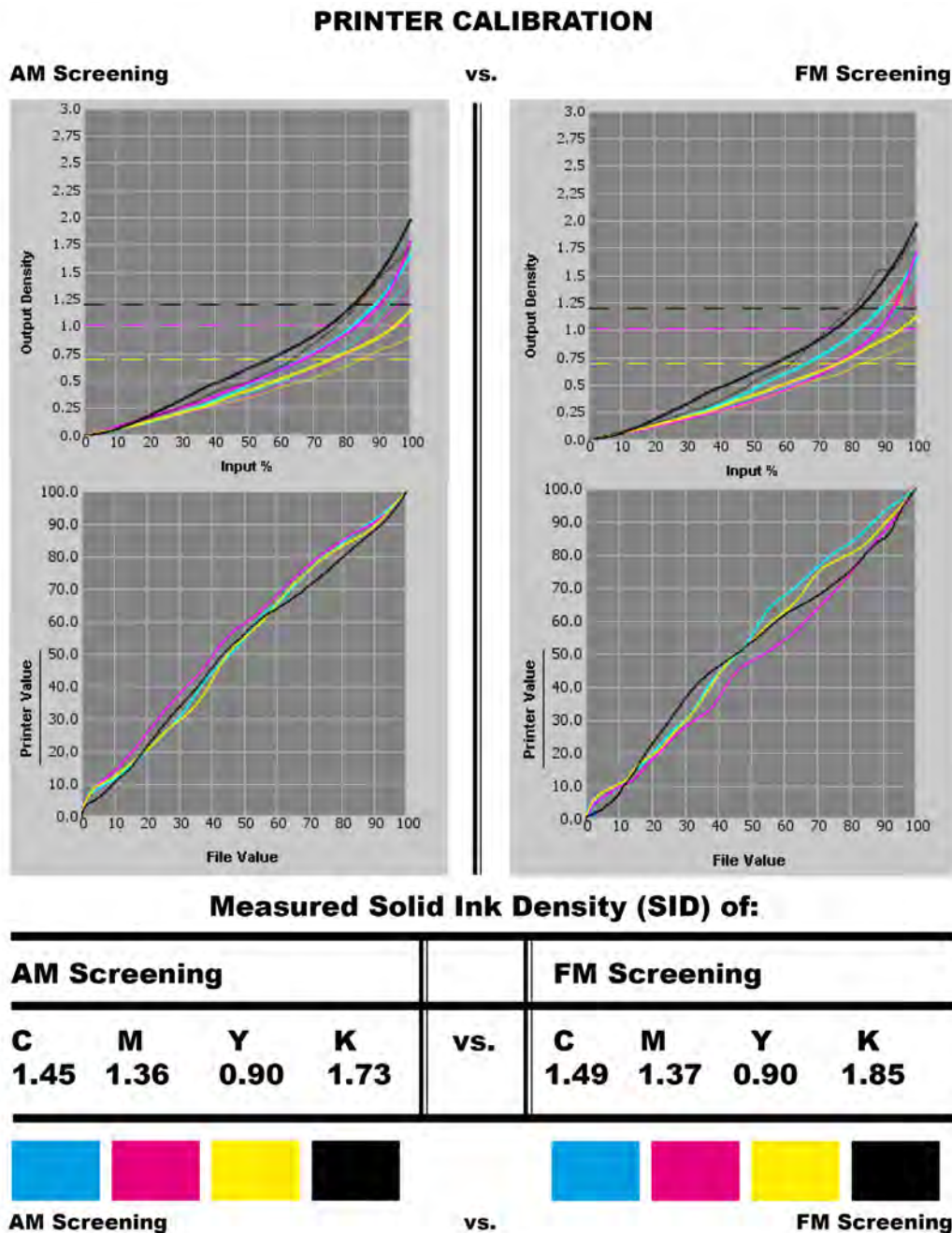
N = the total population size

P = the population proportion that it is desired to estimate (.50)

d = the degree of accuracy expressed as a proportion (.05)

G7 Compliance for Digital Color Press (printer)

Prior to printing the patches/target image, the printer was calibrated for both the screening options (AM and FM) according to its manufacturer specifications. A calibration process means standardizing the performance of the devices according to the device manufacturer specifications so that the results of the devices are repeatable. The calibration curve consists of the maximum printable densities of each color (CMYK) of both the screening techniques (See Figure 4). Test target TC1617x was used for the output device profile creation process.



» Figure 4: Calibration of AM vs. FM Screening

In a generic color managed digital printing workflow, digital front-end (DFE) platforms (raster image processor or RIP) of digital printers (or presses) offer opportunities for the user (or press operator) to manipulate the output color quality to meet the expected demand of the customer. In order to print a quality halftone image, the user must carefully manage several print parameters, variables, and attributes which are associated with the digital printing process. For this experiment, printer resolution was reduced to 600 dots per inch (DPI) because one screening option (FM screen) in the front-end platform (RIP) was limited to only this setting. This is due to random micro-dot placement, without use of screen angles, for the dot reproduction of FM screening. However, the AM screening option offered the ability to set printer resolution at 600 DPI, 1200 DPI, and 2400 DPI. In order to test the screening effect on the digital color output (DCO) only the 600 DPI resolution was selected for both screening technologies to keep the parameters/variables consistent throughout the experiment. Table 1 presents the variables, materials, conditions, and equipment associated with this experiment.

Output Device Profiles (ODP) with AM and FM Screening for G7 Compliance

The target image (TC1617x) was placed into an Adobe InDesign-CC layout of 12" W x 18" H size and a .PDF file was created without any image/color compression

technique (see Figures 3 & 3A). Hammermill brand, 100 LB matte-coated digital color printing paper 12" x 18" was used for printing the samples in the experiment. Prior to printing the TC1617x target (See Figure 3A) for creating the device profile, the printer was calibrated. The calibration data (range of CMYK densities) were saved in the calibration lookup tables of the RIP and a calibration curve was created. A total of 100 sheets/copies of TC1617x were printed with the calibration curve attached. Also, an amplitude modulated (AM) halftone screening technique with 190 lines per inch (LPI) and 600 DPI as the printer resolution was applied during the printing. No color management or color correction techniques were applied during the printing.

Printed patches of TC1617x were measured in CIE L* a* b* space using the i1PROFILER application with an X-Rite spectrophotometer with an i1iO table and the data were run through this application. The printer profile was created and stored at the right location on the computer. The profile format version is 4.00 and it is considered as the Output Device Profile (ODP) of AM screening. This profile was used as a destination profile (DP) in the workflow. The source profile (SP) used in the experiment is a GRACoL2013 for characterized reference printing conditions-6 (CRPC-6). *The same procedures as described above in this section were followed for creating the ODP for FM screening with an FM screened calibration curve and the 600 DPI as the printer resolution.*

Table 1

Experimental and Controlled Variables

Variable	Material/Condition/Equipment
Test image	Custom Test Target, 2 pages
Control strips/targets	ISO 12647-7 (2013), TC1617x
Other Images	B/W and Color for Subjective Evaluation
Profiling Software	X-Rite i1PROFILER 1.8
Profile Inspection Software	Chromix ColorThink-Pro 3.0
Image Editing Software	Adobe PhotoShop-CC
Page Layout Software	Adobe InDesign-CC
Source Profile (RGB)	Adobe 1998.icc
Destination Profile (CMYK)	Custom, Konica-Minolta.icc
Reference/Source Profile (CMYK)	GRACoL2013.icc
Color Management Module (CMM)	Adobe (ACE) CMM
Rendering Intents	Absolute
Computer & Monitor	Dell OPTIPLEX/LCD
Raster Image Processor (RIP)	Creo IC-307 Print Controller
Printer	Konica-Minolta bizHub C6000 Color Laser
Achieved CMYK SID for all print runs (AM vs. FM)	C = 1.47; M = 1.37; Y = 0.90; and K = 1.79
Screens and Screen Ruling	AM & FM, 190 LPI for AM
Print Resolution	600 x 600 DPI
Toner	Konica-Minolta Color Laser
Type of Paper Weight/thickness	Hammermill 100LB Matte Coated, Sheetfed
Type of Illumination/Viewing Condition	D50
Color Measurement Device(s)	X-Rite Eye-One PRO Spectrophotometer with Status T, 2° angle, and i1iO Scanning Spectrophotometer
Data Collection/Analysis Software	Chromix/IDEAlliance Curve 4.0 & MS-Excel

See Figure 5 for all output device profiles comparison (GRACoL 2013, AM vs FM Screened) with profile volume (gamut volume) and L* a* b* values of each profile used.

Printing for G7 Compliance

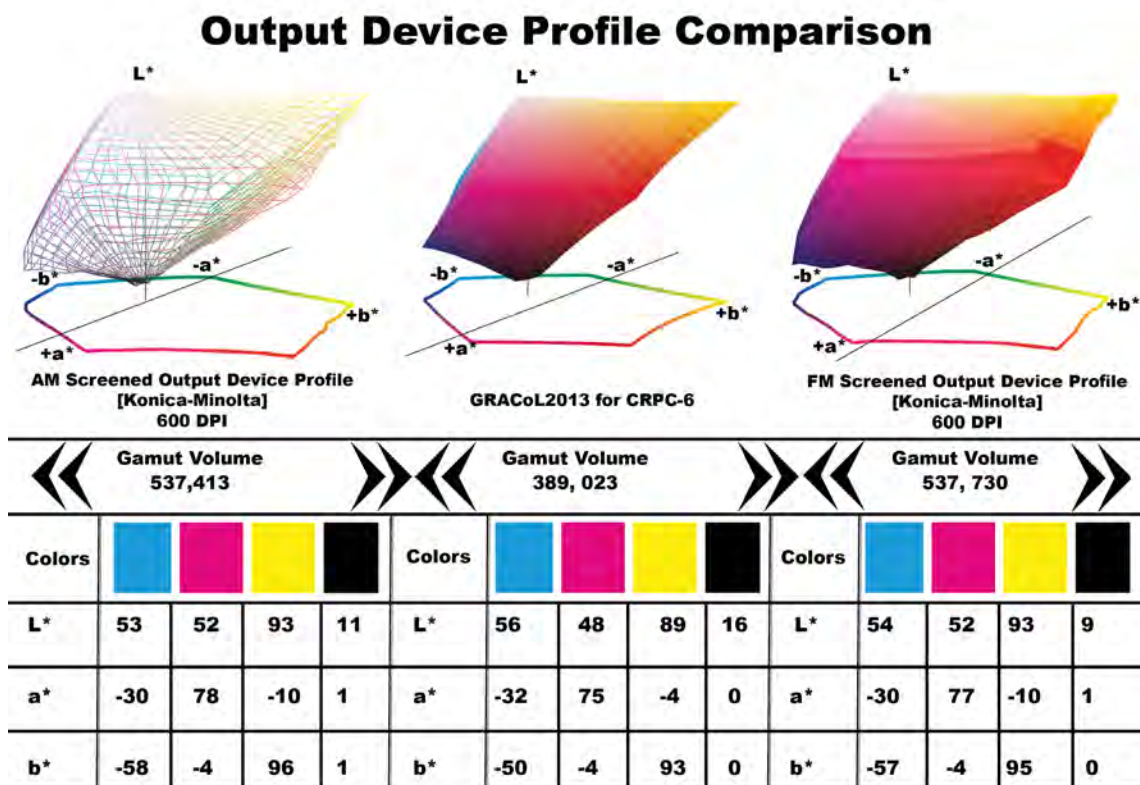
Each screening technique (AM or FM) used in the experiment (see Figure 6) was considered as a group, noted by letter “K” (K = 2). A group involves a set of print parameters, such as: a digital halftone screening technique [amplitude modulate (AM) **OR** frequency modulate (FM)], the calibration curve (AM **OR** FM screened), a color source profile [General Requirements for Applications in Commercial offset Lithography for characterized reference printing conditions (GRACoL2013 for CRPC-6)], and a color destination profile of a digital press (AM **OR** FM screened). As parameters illustrated in Figure 6 (*Schematic Illustration of Sequence of Print Parameters for G7 Compliance*), test target of 12” x 18” was printed for use in the experiment. The test target contained the following elements: TC1617x target, ISO 12647-7 (2013) control strips, an ISO 300 and custom images of color and b/w for subjective evaluation of color. A total of 100 sheets/samples were printed for each screening technique by enabling the color management technique at the RIP. The digital press AM or FM calibration curve, AM or FM screening destination profile, and the source profiles all were applied during the printing (see Figure 6).

Press Run 1: Printing with ODP of AM Screening

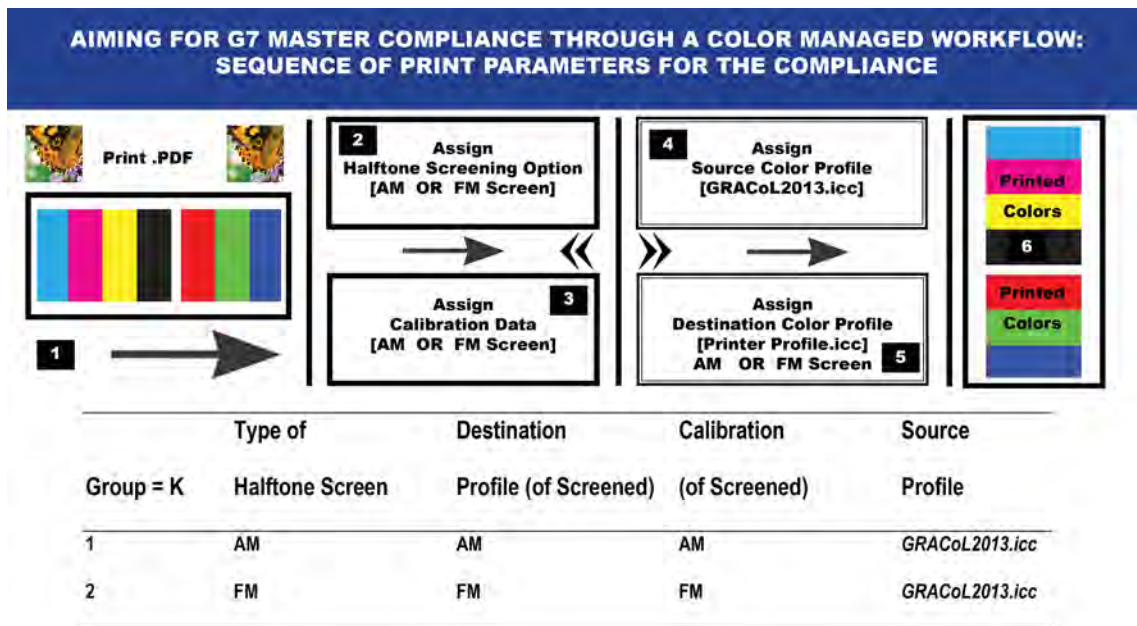
A total of 100 sheets/samples were printed (See Figure 6). The digital press calibration curve (AM Screened), AM screening destination profile, and the source profile (GRACoL 2013) all were applied during the printing. A total of 80 randomly pulled printed copies of TC1617x printed target images were measured against G7 ColorSpace GRACoL 2013 (CGATS21-2-CRPC6) in CIE L* a* b* space using an IDEAlliance (Chromix/Hutch Color) Curve 4.2.4 application interface with an X-Rite spectrophotometer with an i1iO table. The measured data were combined/averaged to run through this application (Curve 4.2.4). The combined data set was analyzed by using the Verify Tool of the application to determine the pass/fail of G7 master compliance levels using G7 ColorSpace tolerances. Analyzed data from the experiment revealed that the printed colorimetric values (G7 Grayscale, G7 Targeted, and G7 Colorspace) are in match with the G7 master compliance levels (reference/target) colorimetric values (G7 Grayscale, G7 Targeted, and G7 Colorspace).

Press Run 2: Printing with ODP of FM Screening

A total of 100 sheets/samples were printed (See Figure 6). A total of 100 sheets/samples were printed by enabling the color management technique for the use of ODP of FM screening at the RIP. The digital press



» Figure 5: Output Device Profiles Comparison



» **Figure 6:** Schematic Illustration of Sequence of Print Parameters for G7 Compliance

FM screened calibration curve and the resolution both were applied during the printing. A total of 80 randomly pulled printed copies of TC1617x printed target images were measured against G7 ColorSpace GRACoL 2013 (CGATS21-2-CRPC6) in CIE L* a* b* space using an IDE-Alliance (Chromix/Hutch Color) Curve 4.2.4 application interface with an X-Rite spectrophotometer with an i1iO table. The measured data were combined/averaged to run through this application. Color measurement and analysis steps used in the *printing with ODP* process AM screening (previous section) were applied/ followed for printing with the FM screening printing process. Printed colors with ODP of FM screening were also found to be very accurate and efficient.

Data analysis & research findings

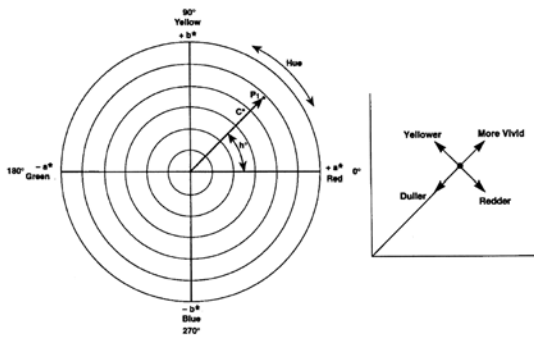
The colorimetric computation methods for G7 compliance were used to analyze the collected data and presented in the following pages/tables. Subjective judgment on color difference or any deviation was not used in this study. The subjective judgment of color difference could differ from person to person. For example, people see colors in an image not by isolating one or two colors at a time (Goodhard & Wilhelm, 2003), but by mentally processing contextual relationships between colors where the changes in lightness (value), hue, and chroma (saturation) contribute independently to the visual detection of spatial patterns in the image (Goodhard & Wilhelm, 2003). Instruments, such as colorimeters and spectrophotometers, could eliminate the subjective errors of color evaluation perceived by human beings. In comparing the color differences between two colors, a higher

deviation (ΔE or ΔH or the ΔC) is an indication that there is more color difference and a lesser deviation (ΔE or ΔH or the ΔC) is an indication of less color difference.

The data for each screening group were generated from the printed TC1617x target image (see Figure 3A) by using an Eye-One-Pro spectrophotometer with an interface application, such as the IDEAlliance Curve 4.2.4 against the GRACoL2013_CRPC6 reference data. The test chart (TC) 1617x is a new CMYK printer characterization target combining the unique patch values in the standard IT8.7/4 target with all the patch values in columns 4 and 5 of the P2P51 target. The letter “x” distinguishes the final version from earlier prototype versions circulated during development. The TC1617x maintains the same patch count as the IT8.7/4 (1,617 – hence the name is TC1617x) by removing 29 duplicate patches from the IT8.7/4 and replacing them with the 29 patches in columns 4 and 5 of the P2P51 that were absent in the IT8.7/4. Data derived from the TC1617x target image is the difference between the characterization data set (TC1617x) and the printed sample. The reference file content for this image (TC1617x) is the CMYK dot percentage values and nominal CIE L* a* b* characterization data values for the GRACoL2013-CRPC6 reference. Analyzed G7 master compliance levels (reference/target) data (G7 Grayscale, G7 Targeted, and G7 ColorSpace) with G7 colorimetric formulae and formats were presented in the following sections for each of the levels.

CIE L* a* b*, Delta L* Delta E and Delta Chroma (ΔL, ΔE and ΔC)

Colorimetric values of printed colors against original colors and the deviations (Deltas) can be used to determine the visual variation in overall colors, hue, chroma, and lightness. The a*, b* coordinates correspond approximately to the dimensions of redness – greenness and yellowness – blueness respectively in the CIE L* a* b* color space and are orthogonal to the L* dimension. Hence a color value whose coordinates a* = b* = 0 is considered achromatic regardless of its L* value. Calculation of ΔH* requires colorimetric data from the L* a* b* model.



» **Figure 7:** Schematic of L* a* b* & c*, h* Coordinates

Metric hue angle h* and C* are defined by the following formulas (Morovic, Green, & MacDonald, 2002).

$$h^*_{ab} = \tan^{-1} \left(\frac{b^*}{a^*} \right) \quad (2)$$

Where: a*, b* are chromaticity coordinates in L* a* b* color space

$$\text{Chroma (C}^*) = [a^2 + b^2]^{1/2} \quad (3)$$

Where: a*, b* are chromaticity coordinates in L* a* b* color space

Calculation of ΔC* (of two colors) and ΔL* requires colorimetric data from the L* a* b* model. Difference in the chroma C* of two colors (Reference vs. Printed) can be calculated by using the following formula (Green et al., 2002).

$$\Delta\text{Chroma (}\Delta\text{C)} = C^*_1 - C^*_2 \quad (4)$$

Where: 1 = C* of Reference Color and 2 = C* of Printed Color

Assessment of color is more than a numeric expression. It is an assessment of the difference in the color sensation (delta) from a known standard. In the CIELAB color model, two colors can be compared and differentiated. The expression for these color differences is expressed as ΔE (Delta E or Difference in Color Sensation). The fol-

lowing equation is used to calculate the ΔE (Committee for Graphic Arts Technologies Standards – CGATS, 2003)

$$\Delta E^* = \sqrt{(L_1 - L_2)^2 + (a_1 - a_2)^2 + (b_1 - b_2)^2} \quad (5)$$

Where: 1 = Reference Color and 2 = Printed Color

Chromaticness difference (ΔCh) is the difference between the reference chroma (a*₁ and b*₁) and the measured chroma (a*₂ and b*₂) of a gray balance control patch (C50, M40, Y40). Weighted Delta Chroma (wΔCh) is the delta Ch value after it is passed through a weighting curve that reduces the significance of Ch errors in the darker regions of the color. The weighting function is defined in the G7 specifications ([Technical Report (TR) 015] and the G7 master pass/fail document as follows (Chromix, Inc., 2019):

$$w\Delta\text{Ch} = \Delta\text{Ch} \times [1 - \max(0, (\% - 50) / 50 \times 0.75)] \quad (6)$$

Delta L* (ΔL*) is the difference in the lightness between the reference and measured sample lightness regardless of any color. This makes ΔL* the perfect metric for measuring tonality [Neutral Print Density Curve (NPDC)] error in G7. Colorimetrically, ΔL* is the result of subtracting the L* of measured sample value from the reference L*, as follows:

$$\Delta L^* = L^*_1 - L^*_2 \quad (7)$$

Where: 1 = L* of Reference Color and 2 = L* of Printed Color

Weighted Delta L* (wΔL*) is the delta L* value after it is passed through a weighting curve that reduces the significance of L* errors in the darker regions of the color. The weighting function is identical to that for wΔCh, as follows (Chromix, Inc., 2019):

$$w\Delta L^* = \Delta L^* \times [1 - \max(0, (\% - 50) / 50 \times 0.75)] \quad (8)$$

Overall Color Variation (ΔE) of AM Screened (TC1617x image) vs. GRACoL 2013 Ref.

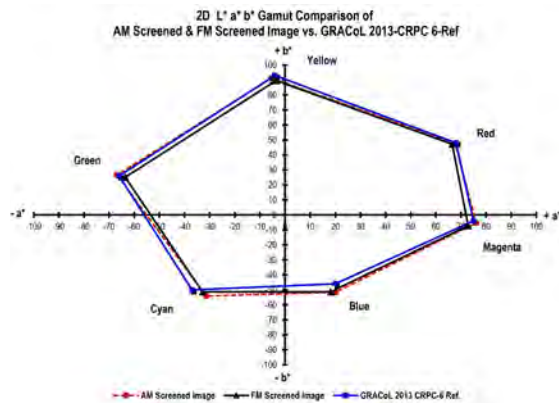
The CIE L* a* b* values associated with the CMYK+RGB colors AM screened image vs. G7 ColorSpace-GRACoL 2013 [CGATS21-2-CRPC6 (reference)] are compiled in Table 2. Numerical color differences (ΔE) were found when comparing the colors of an AM screened printed image vs. G7 ColorSpace at all seven colors (CMYK+RGB). Also, noticeable visual color differences were found in the solid color area [lightness, color hue and chroma]. Overall, both groups of images have similar colors (See Figure 8) with the exception of the printed image consisting of higher L* for red, magenta, and green, etc. This results in producing the higher ΔE for these colors.

Table 2

Overall Color Variation of CMYK+RGB: AM Screened Image (TC1617x) vs. G7 ColorSpace

Color(s)	AM Screened Image			G7 ColorSpace / Target			Color Difference ΔE
	L*	a*	b*	L*	a*	b*	
	Color 1 N = 80			Color 2 N = N/A			
White (W)	97.22	2.79	-9.47	97.22	2.79	-9.47	0.00
Cyan	57.44	-31.3	-54.11	57.39	-36.88	-55.85	1.99
Magenta	51.49	76.06	-5.38	49.21	77.92	-7.10	2.40
Yellow	90.98	-5.36	91.29	91.09	-2.44	92.91	1.62
Black (K)	13.46	0.34	-0.11	16.30	0.24	-0.74	1.97
Red	50.64	67.72	47.65	48.19	70.73	48.27	2.59
Green	53.39	-66.80	26.68	51.25	-66.87	24.48	2.29
Blue	26.79	20.05	-51.57	25.62	21.18	-50.24	1.60
TAC 300	24.33	-0.07	-1.73	23.56	0.45	-1.35	1.02
TAC 400	9.74	0.55	-0.97	8.99	0.17	0.61	1.72

This higher color deviation (red, magenta, and green) could be the result of the substrate (paper) and inks used (age, condition, quality, etc.). These are the darker colors which produced lower L* value and, in turn, affected the higher deviation. The 2D color gamut comparison (see Figure 8) reveals that the colors of the printed image closely match the reference colors. The goal was to determine the deviations among various attributes of color between these two groups of colors. The comparison is an indication that, in a color managed workflow (CMW), color matching of a target image can be achieved from device to device regardless of device color characterization and original colors. Subjective judgment was not used for the color comparison.



» **Figure 8:** AM Screened and FM Screened Image vs. GRACoL 2013-CRPC-6 Ref.

Overall Color Variation (ΔE) of FM Screened (TC1617x image) vs. GRACoL 2013 Ref.

The CIE L* a* b* values associated with the CMYK+RGB colors FM screened image vs. G7 ColorSpace-GRACoL 2013 [CGATS21-2-CRPC6 (reference)] are compiled in

Table 3. Numerical color differences (ΔE) were found when comparing (See Figures 8) the colors of the FM screened printed image vs. G7 ColorSpace at all seven colors (CMYK+RGB). Also, noticeable visual color differences were found in the solid color area [lightness, color hue and chroma]. Overall, both groups of images have similar colors with the exception of the printed image consisting of higher L* for red, green, and blue, etc. This results in producing the higher ΔE for these colors. See Figure 9 (scanned printed images) for visual comparison of the printed colors of the screening method applied.



» **Figure 9:** AM Screened Printed vs. FM Screened Printed Images (colors)

This higher color deviation (red, green, and blue) could be the result of the screening technique applied. These are the darker colors which produced lower L* value and, in turn, affected the higher deviation. The 2D color gamut comparison (see Figure 8) reveals that the colors of the printed image closely match the reference colors. The goal was to determine the deviations among various attributes of color between these two groups of colors. The comparison is an indication that, in a color managed workflow (CMW), G7 master compliance for color matching of a target image can be achieved. Subjective judgment was not used for the color comparison.

In addition to the colorimetric comparison of individual colors (Tables 3 and 4) of both screening groups with G7 ColorSpace, the G7 master compliance colorimetric deviation ($w\Delta Ch$ and

Table 3

Overall Color Variation of CMYK+RGB: FM Screened Image (TC1617x) vs. G7 ColorSpace

Color(s)	FM Screened Image			G7 ColorSpace / Target			Color Difference ΔE
	L*	a*	b*	L*	a*	b*	
	Color 1 N = 80			Color 2 N = N/A			
White (W)	97.03	2.87	-9.98	97.03	2.87	-9.98	0.00
Cyan	56.34	-32.82	-51.34	57.27	-36.77	-56.22	1.87
Magenta	50.06	72.88	-7.15	49.11	77.85	-7.38	1.48
Yellow	89.73	-3.57	89.57	90.92	-2.35	92.53	1.17
Black (K)	15.73	0.05	0.47	16.28	0.26	-0.81	1.35
Red	50.65	66.50	47.19	48.09	70.67	48.07	2.82
Green	53.96	-63.60	25.14	51.15	-66.70	24.22	2.95
Blue	27.49	18.13	-51.30	25.57	21.16	-50.44	2.76
TAC 300	24.30	-0.28	0.53	23.51	0.47	-1.47	2.31
TAC 400	10.63	0.44	0.21	8.99	0.16	0.62	1.17

Table 4

G7 Master Compliance Levels G7 Grayscale of AM Screen, FM Screen vs. G7

All Metrics	Black (K)	CMY (Overlap)		G7 Tolerance
	w ΔL^*	w ΔL^*	w ΔCh	
G7 Grayscale of AM Screened Image (Tonality/Gray Balance)				
Average	0.90	0.39	0.89	1.50
Maximum	2.37	1.18	1.72	3.00
G7 Grayscale of FM Screened Image (Tonality/Gray Balance)				
Average	0.91	0.89	1.12	1.50
Maximum	2.16	1.92	2.4	3.00

Table 4A:

G7 Master Compliance Levels G7 Targeted of AM Screen, FM Screen vs. G7

All Metrics	ΔE 2000	G7 Tolerance	Maximum	G7 Tolerance
G7 Targeted of AM Screened Image				
Substrate	0.00	3.00		
K	1.97	5.00		
CMY			2.40	3.5
RGB			2.59	4.3
G7 Targeted of FM Screened Image				
Substrate	0.00	3.00		
K	1.35	5.00		
CMY			1.87	3.5
RGB			2.95	4.3

Table 4B:

G7 Master Compliance Levels G7 Colorspace of AM Screen, FM Screen vs. G7

All Metrics	ΔE 2000	G7 Tolerance
G7 Colorspace of AM Screened Image		
Average	1.28	3.5
95%	2.33	5.0
G7 Colorspace of FM Screened Image		
Average	1.71	3.5
95%	3.53	5.0

w ΔL) values for all the three levels (G7 Grayscale, G7 Targeted and G7 Colorspace) are in close match with the established tolerances for the G7 (see Table 4, 4A, and 4B) including the Neutral Print Density Curve [NPDC (CMY)] and NPDC (K).

Summary/Conclusions

This experiment used an output device ICC profile to achieve the compliance. G7 master compliance includes three compliance levels in the G7 master qualification: G7 Grayscale, G7 Targeted, and G7 Colorspace. These levels demonstrate G7 master capabilities of

a print facility. The experiment was conducted in a Color Managed Digital Printing Workflow (CMDPW). It was aimed at achieving the G7 master compliance through an ICC based color managed workflow (CMW). The G7 calibration method, using the P2P251x target, was **NOT** used to derive the device NPDC to compare with G7 NPDC for print (or press) runs 1, 2, 3, etc.

The conclusions of this study are based upon an analysis of colorimetric data, visual assessment, and associated findings. The experiment analyzed the comparison of G7 compliance of two screening technologies. The guiding objectives of this study allowed testing of an

accepted color management practice to gain a better understanding of the presumptions associated with the application of an output device profile (ODP). The experiment examined the importance of calibration, characterization and the color evaluation processes of the digital press which was capable of printing colors to match or be in proximity of G7 master compliance levels.

It is evident that integration of device profiles is important in a CMW and it also enables/allows the workflow process to meet the G7 compliance levels via an ICC based CMW, instead of using G7 calibration methodology. Selection of screening method is based on individual preference because both screening options proved to be within the G7 compliance. This study represented specific printing or testing conditions. The images, printer, instrument, software, and paper that were utilized are important factors to consider when evaluating the results. The findings of the study cannot be generalized to other digital printing workflow. However, other graphic arts educators, industry professionals, and researchers may find this study meaningful and useful.

References

- Chromix, Inc. (2019) *Curve 4.2.4 Software Manual*. Seattle, Chromix, Inc.
- Chung, R. & Ma, L. L. (1995) Press Performance Comparison between AM and FM Screening. TAGA Proceedings 1995, Rochester, New York, TAGA.
- Committee for Graphic Arts Technologies Standards-CGATS (2003) *Graphic technology – spectral measurement and colorimetric computation for graphic arts image*. (ANSI/CGATS.5-2003). Reston, The Association for Suppliers of Printing and Publishing Technologies, p.29.
- Fleming, P., Dollak, J. & Fryzlewicz, S. (2008) Stochastic Screening: What to do When Your Rip Doesn't Support It and Comparison with Conventional Screening on an Offset Press. *Journal of Graphic Technology*. 1 (3), 15-23
- Glass, G. V. & Hopkins, K. D. (1996) *Statistical Methods in Education & Psychology*. Boston, Allyn & Bacon.
- Goodhard, M. M. & Wilhelm, H. (2003) *A new test method based on CIELAB colorimetry for evaluating the permanence of pictorial images*. Wilhelm Imaging Research, Inc. Available from: <http://www.wilhelm-research.com> [Accessed: 20th August 2019].
- International Digital Enterprise Alliance- IDEAlliance (2014) *IDEAlliance Guide to Print Production*. Alexandria, IDEAlliance.
- Ma, L.L. (2003) Understanding Digital Halftones. *Journal of Visual Communications*. 130-136.
- Morovic, J. (2002) Colour gamut mapping. In: Green, P. & MacDonald, L. (eds.) *Colour Engineering Achieving Device Independent Colour*. New York, John Wiley & Sons, pp. 297-314
- Novaković, D. & Avramović, D. (2012) Influence of Printing Surface Attributes on Print Quality in Electrophotography. *Technical Gazette*. 19 (2), 295-301.
- Pnueli, Y. & Bruckstein, A. (1996) Gridless Halftoning: A Reincarnation of the Old Method. *Graphical Models and Image Processing*. 58 (1), 38–64. Available from: doi: 10.1006/gmip.1996.0003
- Wales, T (2009) Paper: The Fifth Color. In: *IPA Bulletin*. Alexandria, IDEAlliance.



© 2021 Authors. Published by the University of Novi Sad, Faculty of Technical Sciences, Department of Graphic Engineering and Design. This article is an open access article distributed under the terms and conditions of the Creative Commons Attribution license 3.0 Serbia (<http://creativecommons.org/licenses/by/3.0/rs/>).


The effect of electromagnetic radiation on the reflectance spectra of prints on hemp papers

ABSTRACT

From the moment of production, paper as a printing substrate is exposed to the process of natural ageing regardless of the type of cellulose fibres in its composition. Accordingly, the prints produced by the various printing techniques are also exposed to several factors that impair the quality of the print i.e. its colour over time. Therefore, it is very important to properly select the printing substrate for achieving a high quality of graphic products. For that purpose, three types of papers with hemp fibres were used as printing substrates which were printed with laboratory hand-operated instrument Esiproof using flexographic cyan (C), magenta (M), yellow (Y) and black (K) water-based inks. Prints were artificially aged in SunTEST XLS+ test chamber according to standard ASTM D 6789-02 for 48 and 96 hours. Based on changes in the reflectance spectra of each printed ink after exposure to electromagnetic radiation it was noticed how composition of printing substrate strongly influence on colour stability of prints due time. An increase of exposure time to electromagnetic radiation leads to a decrease in the value of the reflectance of the printing substrate and cyan, magenta and yellow prints. It was confirmed how electromagnetic radiation have the greatest impact on the reflectance of yellow print, while the black one is the most stabile regardless of the substrate it was printed on.

KEY WORDS

Artificial ageing, flexographic inks, hemp, paper, reflectance spectra

Ivana Plazonić 
Vesna Džimbeg-Malčić 
Irena Bates 
Gabriel Žilić

University of Zagreb,
Faculty of Graphic Arts, Zagreb, Croatia

Corresponding author:
Ivana Plazonić
e-mail: ivana.plazonic@grf.unizg.hr

First received: 2.2.2021.

Revised: 24.2.2021.

Accepted: 22.3.2021.

Introduction

Industrially grown hemp (*Cannabis sativa* L.) is a plant that has been recognized as an important raw material for many industries, including the paper industry (Danielewicz & Surma-Ślusarska, 2010; Miao et al., 2014). This plant features strong and long fibres with low lignin content. In total, 35% of fibres are classified as long bast fibres, and 65% are short core fibres. Hemp fibre for paper production must have a fibre length of 15-55 mm (Azeez, 2018). An important feature of this raw material is also the time of growth required after which it can supply the paper industry. It is known that the wood is the main raw material for pulp and paper industry and 20-80 years are required for trees growth to provide fibres for paper production. On the other hand, hemp can reach a height of 4-5 meters in only 80-150 days when it is clas-

sified as mature for fibre harvesting. Compared to one hectare of forest, one hectare of hemp can produce four times more paper (Małachowska et al., 2015). However, hemp as a fast-growing alternative to trees is annual plants which results in some disadvantages. Due to the macroscopic structure, there are great differences along the plant from top to bottom in terms of morphological structure and chemical composition. The disadvantages of hemp woody-core pulp and hemp bast fibre pulp as papermaking intermediates proved to be low tear resistance and low tensile strength, respectively. The main reasons for the low tensile strength of hemp bast fibre pulp are the low susceptibility of their fibres for internal fibrillation and low hemicellulose content (Danielewicz & Surma-Ślusarska, 2017). Regardless of the origin of the cellulose fibres used in the paper industry, paper as a product is subjected to a process of natural ageing.

This irreversible chemical and physical process occurs slowly over time in all papers from the moment of its production. It involves numerous interactions between substances in the paper and with its surroundings (Radkova et al., 2015; Černič Letnar & Kropar Vančina, 2002), causing structural changes and chemical composition of the material leading to the changes in the functional properties of material (Žoček-Tryznowska & Annusik, 2019). Therefore, the samples produced by the printing on the paper substrates are also exposed to several factors that impair the print quality i.e. its colour over time. These changes are mainly observed as a fading of colours on prints. So, it is particularly important to select the printing substrate which will provide the required quality of graphic products due time. The stability of paper and prints during the ageing process is largely determined by composition of the paper, printing ink and their interaction during printing process. To evaluate the permanence of paper or print different methods of accelerated/artificial ageing have been used by researchers all over the world. These methods include aggravated conditions of heat, humidity, oxygen, sunlight, vibration, etc. to speed up the normal ageing processes of items. UV radiation is the primary cause of degradation in inks, in combination with temperature and moisture acting as secondary stressors that can accelerate the rate of degradation (Lind et al., 2004). Namely, light as a visible part of spectrum is divided into ultraviolet light (UV), visible light, and infrared energy (IR) that have the shortest to the longest wavelength, respectively. UV light has the highest energy among the electromagnetic spectrum because the short wavelength exhibits higher energy due to the higher frequency of the waves at the same speed of light in space. UV light breaks the chemical bonds of molecules in objects, including colour of printed materials. The molecules of the colour absorb UV light and activate a chemical reaction of electrons leading to photochemical degradation, while the degradation visually affects colour degradation or colour fading (Narakornpijit, 2018). However, artificial ageing of paper can just partially simulate the natural ageing mechanisms such as hydrolysis, oxidation, and photodeterioration (Zervos, 2010).

In our previous research (Plazonic et al., 2020b; Plazonic et al., 2018) results indicate that hemp fibres can produce high-quality office papers that are more stable under light and temperature influences than those made with post-consumer fibres. However, to increase the durability of manufactured papers, hemp fibres must be bleached. However, the composition of paper as a printing surface is only one of the factors that ensure the quality of the printed graphic product. Another factor is the chosen printing technique, as well as the ink that will interact with the printing substrate, but the negative impact of external climate conditions to which printed products are often exposed to is extremely important. Generally, black and cyan will fade only slightly, while at the same time yellow and magenta will noticeably

fade. Yellow absorbs visible blue light (450 nm- 495 nm) which has the highest energy of visible electromagnetic radiation, so yellow will show more significant discoloration than other process colours (Narakornpijit, 2018). Ink is structurally a dispersion system consisting of pigment, binder and solvent, and it is proven that with the lower ink pigmentation concentration is the lower the lightfastness (Aydemir, Yenidoğan & Özsoy, 2019). It is important to emphasize that the film thickness of the ink on the surface of the print substrate is highly decisive in light resistance. When the thickness of the ink film increases, the light fastness will be higher as the number of pigments affected by the light in a certain region will increase. Therefore, it is important to maintain a continuous ink thickness during printing (Aydemir & Yenidoğan, 2018). In general, the stability of an ink layer to UV light depends on the exposure of the ink to light, as well as on the thickness, transparency, pigmentation, filler content factors, or white pigment in the ink film (Aydemir et al., 2021). Studies of effect of electromagnetic radiation on the stability of the ink layer on paper substrates are limited, especially in the field of flexographic printing.

The aim of this study was to evaluate the stability of flexographic print on substrates with hemp fibres based on the reflectance spectra measurements after artificial ageing in Suntest XLS+ test chamber which emits visible and near ultraviolet electromagnetic radiation in range from 290 nm to 800 nm.

Materials and methods

Paper as a printing substrate

In this study three types of office papers were used. Their basic characteristics are summarized in Table 1.

Table 1
Characteristics of hemp fibre-based paper used as printing substrates

Type 1	Type 2	Type 3
90 g/m ²	90 g/m ²	90 g/m ²
100% hemp plant fibre	100% hemp plant fibre	25% hemp and 75% post-consumer waste fibres
100% sustainable	100% sustainable	100% sustainable
unbleached	non-chlorine bleached	acid free, chlorine free
uncoated	uncoated	uncoated
handmade	handmade	industrial

In previous research (Plazonic et al., 2016) it was found that paper Type 3 has the highest share of inorganic com-

ponents (6.35% of CaCO₃ and 0.75% of china clay) and consequently the highest share of ash (ash_{525°C} = 7.01%). Papers made only from virgin hemp fibres, papers Type 1 and Type 2, have a low share of ash (ash_{525°C} < 2.4%).

Full tone prints

All papers were cut in dimensions 190 mm x 40 mm and subjected to manual printing using a print tester Esiproof (RK print). The cyan (C), magenta (M), yellow (Y) and black (K) prints were made in full tone by Iroflex 917 inks manufactured by Sun Chemical (Table 2). For producing quality flexographic prints, ceramic anilox roller having 40 lin/cm (60° spread angle) with a total cell volume of 39.10 cm³/m² was used. The purpose of the anilox roller and the doctor blade situated at an angle of 30° with the tangent point of the anilox roll is to transfer an accurate amount of ink to the surface of the printing plate. The printing process was carried out at a temperature of 23°C and a relative humidity of 50%.

To perceive the value of the ink film thickness on hemp papers, the optical ink density (D_i) was determined on all prints by a densitometer eXact, X-Rite (D50/2°). The optical ink density was calculated according to equation 1.

$$D_i = \log \frac{I_0}{I} \quad (1)$$

where: *I* - the light intensity of the light remitted by the ink film in relation to the *I*₀ intensity of light,

*I*₀ - intensity of the light remitted by unprinted laboratory paper.

The effect of electromagnetic radiation on the optical ink density of cyan, magenta, yellow and black print made on hemp papers was also shown through change of the optical ink density (ΔD_i) calculated by equation 2.

$$\Delta D_i = D_{i \text{ before ageing}} - D_{i \text{ after ageing}} \quad (2)$$

where: ΔD_i - change of the optical ink density;

*D*_{*i* before ageing} - the optical ink density of cyan, magenta, yellow and black print measured before ageing;

*D*_{*i* after ageing} - the optical ink density of cyan, magenta, yellow and black print measured after 96 hours of ageing.

Artificial ageing of papers and prints

Papers and prints were cut into strips 60 mm x 90 mm and placed side by side in Suntest XLS+ test chamber, supplied with a daylight filter, which emit visible and near ultraviolet electromagnetic radiation in wavelength range from 290 nm to 800 nm. The procedure of artificial ageing was carried out according to ASTM D 6789-02, during which the level of light intensity was (765 ± 50) W/m², the temperature was kept at 22.6°C and relative humidity was 50%. Exposure to the UV radiation was performed in 2 cycles for 48 hours and in Table 3 is given information about ageing course. UV dose is the product of UV intensity (expressed as energy per unit surface area) and residence time (Feller, 1994) so it can be calculated by equation 3:

$$UV \text{ dose} = I \times t \quad (3)$$

Table 2

Prints

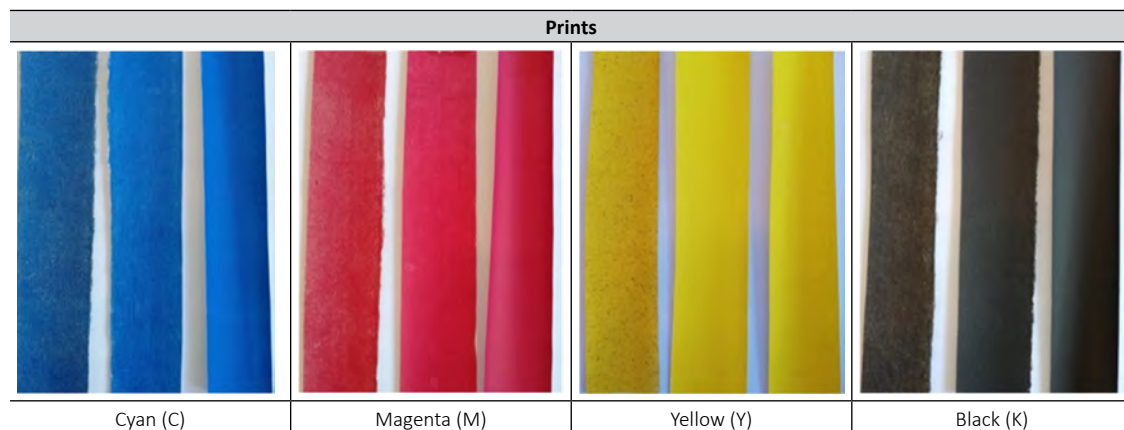


Table 3

Course of ageing in the Suntest XLS+ test chamber

Ageing cycle no.	Time of ageing (h)	Dose of energy supplied (kJ/m ²)	Natural ageing comparable time (days)
1	48	132 192	44.5
2	96	264 384	89.0

where: I - intensity or energy per unit surface area expressed in $J/(cm^2sec)$;
 t - exposure time in sec.

According to the ageing conditions used in this study, every hour spent in the ageing test chamber corresponds a dose of energy absorbed of 2754 kJ/m^2 , which is compatible with approximately 22 hours of natural ageing. This is in correlation with the statement that one hour of treatment under a xenon lamp corresponding to one day in nature (Debeljak & Gregor-Svetec, 2010; Izdebska, Żołek-Tryznowska & Książek, 2013).

Spectrophotometric analysis

Papers and prints reflectance measurements were processed using a spectrophotometer X-rite SpectroEye, in the wavelength interval from 400 nm to 700 nm for every 10 nm. The reflectance measured over white background under illuminant D50 (daylight 5000°K), 2° standard observers, directional geometry, was the basis for the evaluation of optical properties of experimental samples. During the spectrophotometric measurements, the relative humidity of the atmosphere was approximately 60% and the temperature was around 21°C. These measurements were supported by ColorShop 2.0 software and analysed by Technical Graphic Origin 6.0 Professional. The reflectance spectra of all samples before and after artificial ageing for both period of time (48 and 96 hours) was measured, and the results of reflectance measurements are presented as ΔR according to the following equation (4):

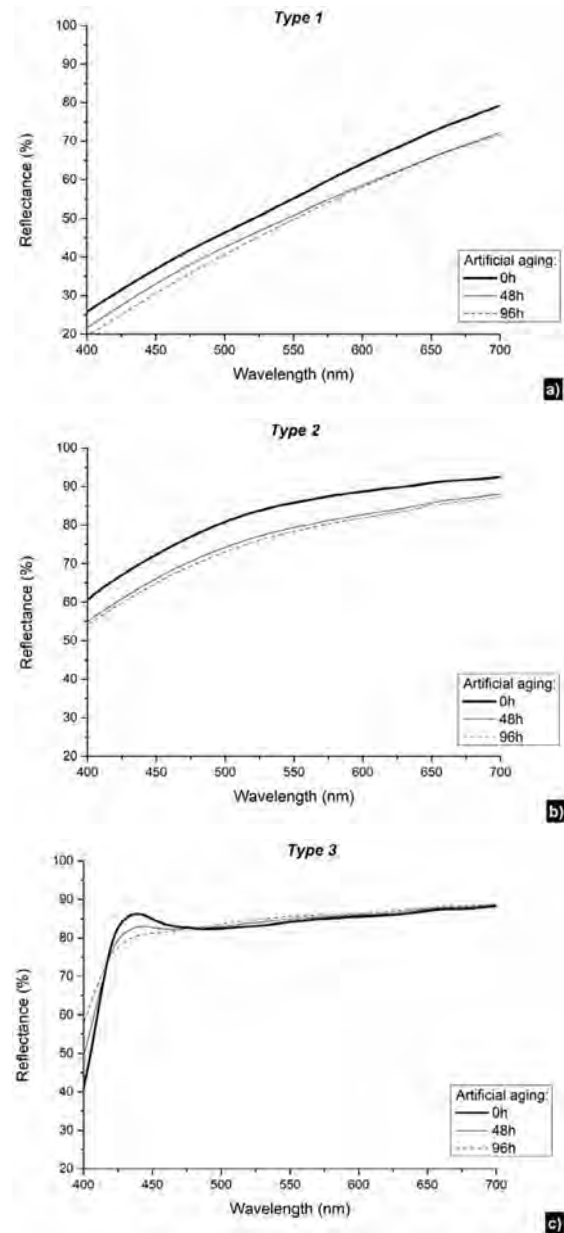
$$\Delta R = R_{\text{before ageing}} - R_{\text{after ageing}} \quad (4)$$

Results and Discussion

Since paper is a complex structure consisting mainly of a network of fibres, filler pigment particles and air, light is not only reflected on paper surface. Within the surface layer, that is, in the paper structure, light also interacts with fibres and pigments. Therefore, in Figure 1 are presented the reflectance spectra for each paper type which are used as a printing substrate.

The spectral reflectance curves shown in Figure 1a-c confirm that papers used in this study as the printing substrate differ greatly in composition. The reflectance curves of paper containing only virgin hemp fibres in their composition are similar (Figure 1a-b), while the reflectance intensity for paper in which the fibres undergo a bleaching process (Type 2) over the entire whole visible part of the spectrum is higher than for paper whose fibres are not bleached (Type 1). This shape of curve is characteristic of pure cellulose/ashless papers such as filter paper (Plazonic, Barbaric-Mikocevic & Dzimbeg-Malcic, 2009). Industrial made

paper with 25% of virgin hemp fibres in its composition and 75% of recycled fibres (Type 3) have a totally different spectral reflectance curve as was expected.



» **Figure 1:** Spectral reflectance curves of the analysed printing substrates: a) paper Type 1; b) paper Type 2; c) paper Type 3

It can be seen from Figure 1c that in addition to bleached paper, this paper also contains a large amount of filler as it intensely reflects light between 420 nm and 480 nm. This shape of the reflectance curve is characteristic for office papers with large amount of fillers as calcium carbonate and clay (Plazonic, Barbaric-Mikocevic & Dzimbeg-Malcic, 2015). By ageing the reflectance of all analysed printing substrates decreases noticeable after 48 h, while further exposure to electromagnetic radiation resulted in a slight decrease in the reflectance. It is also evident that artificial ageing by exposure to electromag-

Table 4

The optical ink density (D_i) of prints and changes in optical ink density (ΔD_i) effected by electromagnetic radiation

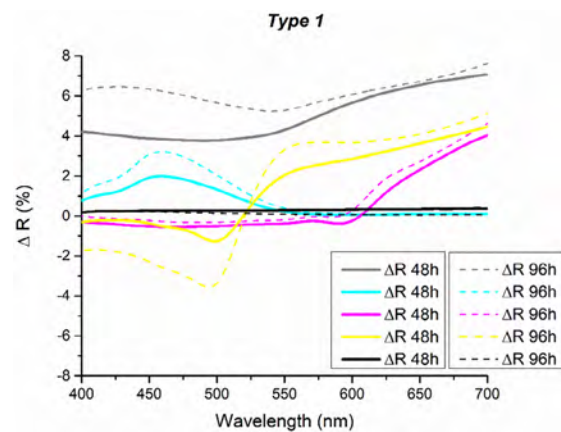
Print	D_i			ΔD_i		
	Type 1	Type 2	Type 3	Type 1	Type 2	Type 3
Cyan	0.99 ± 0.03	1.16 ± 0.02	1.16 ± 0.01	0.04	0.02	0.01
Magenta	1.03 ± 0.05	1.29 ± 0.01	1.22 ± 0.01	0.08	0.07	0.01
Yellow	0.82 ± 0.03	1.13 ± 0.02	1.21 ± 0.01	0.24	0.37	0.25
Black	1.01 ± 0.05	1.32 ± 0.01	1.25 ± 0.01	0.01	0.02	0.00

netic radiation causes approximately the same decrease in the reflectance of both papers with 100% hemp fibre content over the entire whole visible part of the spectrum. For paper Type 3, it was noticed that electromagnetic radiation did not affect the intensity of the spectral reflectance in the visible part of the spectrum in the wavelength range from 480 nm to 700 nm, just in the blue part of spectrum (420 nm – 460 nm). In our previous research where effect of photo-oxidation on the properties of this hemp office papers were analysed, it was founded that hemp fibres can produce high-quality office papers that are more stable against light and temperature influences than those made with post-consumer fibres. Namely, results of strength properties (tensile index, elongation at break, tear index), surface properties (Bendtsen roughness, Bekk smoothness), pH of paper extracts, and optical properties have pointed out that for increasing the durability of manufactured papers, hemp fibres must be bleached. A main purpose of bleaching the pulp is to remove the residual lignin and chromophores inside the pulp, which efficiently absorb UV radiation and cause paper degradation (Plazonić et al., 2020b).

The Type 1 and Type 2 samples are handmade papers, and their smoothness is lower than the smoothness of industrially made paper. However, Type 1 made from unbleached hemp fibres was detected as paper with the roughest surface (Plazonić et al., 2020a). Although the anilox roller provides the transfer of an equal amount of ink to the printing plate, and from the printing plate to the paper, the rougher surface of the paper Type 1 resulted in lower optical ink density for all inks (Table 4). This is because the transferred ink on the rough surface of the paper penetrates the paper after filling the irregular surface (Ha, Park & Kim, 2019). As it is clearly seen from Table 4, the highest effect of electromagnetic radiation after 96 hours was observed on the optical ink density of yellow ink regardless of the composition of paper, while the black ink was the most stable. From the ΔD_i results it is also visible that the prints on industrially made paper (Type 3) are the most stable regardless of the printed ink.

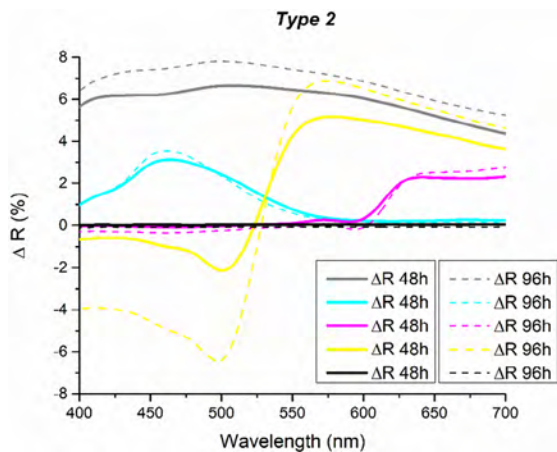
From the differences of reflectance curves between the non-aged and artificial aged specimens shown in Figure 2, it can be seen that the unprinted substrate Type 1 undergoes the greatest reflectance changes due to exposure to electromagnetic radiation across the whole visible part of the spectrum ($\Delta R = 3.9\%$ - 7.9%). It

is also evident that the reflectance values of the printing substrate (on graph marked with grey colour) decrease with increasing the exposure time (from 48 h to 96 h).



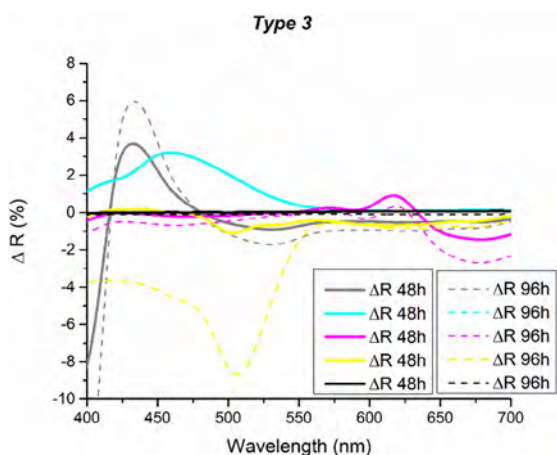
» **Figure 2:** Differences of reflectance spectra measurements before and after artificial ageing of paper Type 1 and of prints on that paper with cyan, magenta, yellow and black inks

On the other hand, prints (on graph each print is marked with similar colour: cyan print with blue colour; magenta print with pink colour; yellow print with yellow; black print with black colour) are far less susceptible to changes in reflectance values than the paper substrate Type 1 on which they are printed. The artificial ageing in general regardless to the exposure time to electromagnetic radiation has no effect on the reflectance of black prints. This is in correlation with the research results provided by Bates, Džimbeg-Malčić & Itrić where spectral changes reflection colour in black offset prints on analysed coated and uncoated papers were insignificant and most likely were influenced by printing ink (Bates, Džimbeg-Malčić & Itrić, 2012) and our previous research (Plazonić et al, 2020b). Other prints (cyan, magenta and yellow) show a change in the reflectance with ageing treatment and the longer the treatment, the greater is the decrease in reflectance values in an area in which a particular colour reflects (cyan in the blue part of the spectrum, magenta in the red part) except for yellow prints which show changes in reflectance throughout the whole visible part of the spectrum. It is evident that yellow prints experience the greatest changes in reflectance due to artificial ageing.



» **Figure 3:** Differences of reflectance spectra measurements before and after artificial ageing of paper Type 2 and of prints on that paper with cyan, magenta, yellow and black inks

Since the composition of the paper Type 2 is identical to the paper Type 1 (only difference is bleaching process before paper formation), Figure 3 shows quite similar reflectance curve shapes with differences in the intensity. It is evident that bleached paper substrate Type 2 undergoes the largest reflectance changes in the whole visible part of the spectrum due to exposure to electromagnetic radiation ($\Delta R = 4.2\% - 7.9\%$). It has been observed that bleached paper Type 2 is also significantly affected by time of ageing where the reflectance of paper is significantly reduces as exposure time increases. All prints are more stable to visible and near ultraviolet electromagnetic radiation than the paper substrate itself. Black prints are unchanged in spectral reflections, while other prints experience a change in reflectance due to artificial ageing, especially yellow prints up to 6.5% after 96 h of ageing.



» **Figure 4:** Differences of reflectance spectra measurements before and after artificial ageing of paper Type 3 and of prints on that paper with cyan, magenta, yellow and black inks

It can be seen from Figure 4 that the industrial made paper Type 3, which contains a much larger amount of recycled than primary hemp fibre and a high amount of fillers, shows greater stability to electromagnetic radiation than other two handmade papers with a 100% hemp fibre content. The only reflectance differences for the paper Type 3 due to artificial ageing were observed in the blue part of the spectrum (maximum value of ΔR is 6% at 430 nm) which is a consequence of high share of fillers in it. Prints on this substrate are also much more stable than prints on handmade papers for both periods of exposure to electromagnetic radiation. The significant influence of electromagnetic radiation after 96 h was noticed only on the reflectance of yellow prints in the blue and green part of the spectrum.

These results of reflectance spectra measurements after artificial ageing of 96 hours are correlated with the optical ink density of prints on hemp apers presented in Table 4.

Conclusions

The aim of this study was to evaluate the usability of hemp fibre based papers for long-term prints. The stability of flexographic prints on such substrates is based on the differences in reflectance spectra for each ageing period. This study has confirmed that the printing substrate significantly influence on the stability of the prints when exposed to electromagnetic radiation. Namely, if the substrate itself is less susceptible to electromagnetic radiation it will provide more stable prints. It is very important to choose the appropriate printing substrate to increase stability of prints, because every paper substrate goes through a degradation process during the time. Interaction between printing substrate and ink are crucial for print stability. Equal transfer of the ink amount to the printing plate and from the printing plate to the paper is enabled by the anilox roller, while the characteristics of the paper surface, such as roughness, reduce the ink thickness, ie the lower optical density ink on the paper. Based on the reflectance spectra of prints on hemp fibre based papers, we concluded that the black print show equal stability to artificial ageing regardless to chemical composition of hemp fibre based papers ($\Delta R < 0.5\%$). The lowest stability on electromagnetic radiation was achieved by yellow prints on all observed substrates (ΔR up to 8.5%). It can also be concluded that with increasing exposure time of electromagnetic radiation reflectance values of printing substrates and cyan, magenta and yellow prints generally decreases.

Acknowledgments

The authors are grateful for the funding provided by the University of Zagreb.

References

- Aydemir, C. & Yenidoğan, S. (2018) Light fastness of printing inks: a review. *Journal of Graphic Engineering and Design*. 9 (1), 37-43. Available from: doi: 10.24867/JGED-2018-1-037
- Aydemir, C., Kašiković N., Horvath C. & Durdevic S. (2021) Effect of paper surface properties on ink color change, print gloss and light fastness resistance. *Cellulose chemistry and technology*. 55 (1-2), 133-139. Available from: doi: 10.35812/CelluloseChemTechnol.2021.55.14
- Aydemir, C., Yenidoğan, S. & Özsoy S. A. (2019) Effects of ink consumption on print quality on coated cellulose-based paper surfaces. *Cellulose chemistry and technology*. 54 (1-2), 89-94. Available from: doi: 10.35812/CelluloseChemTechnol.2020.54.10
- Azeez, A. M. (2018) Pulping of Non-woody Biomass. In: Kazi, S. N. (ed.) *Pulp and Paper Processing*. London, United Kingdom, IntechOpen, pp. 55-87. Available from: doi: 10.5772/intechopen.79749
- Bates, I., Džimbeg-Malčić, V. & Itrić, K. (2012) Optical deterioration of samples printed with basic Pantone inks. *Acta graphica, Journal for Printing Science and Graphic Communications*. 23 (3-4), 79-90.
- Črnič Letnar, M. & Kropar Vančina, V. (2002) The Effect of Accelerated Ageing on Graphic Paperboards Degradation. *Restaurator*. 23, 118-132. Available from: doi: 10.1515/REST.2002.118
- Danielewicz, D. & Surma-Ślusarska, B. (2010) Processing of Industrial Hemp into Papermaking Pulps Intended for Bleaching. *Fibres & Textiles in Eastern Europe*. 18 (6 (83)), 110-115.
- Danielewicz, D. & Surma-Ślusarska, B. (2017) Properties and fibre characterisation of bleached hemp, birch and pine pulps: a comparison. *Cellulose*. 24, 5173-5186. Available from: doi: 10.1007/s10570-017-1476-6
- Debeljak, M. & Gregor-Svetec, D. (2010) Optical and Color Stability of Aged Specialty Papers and Ultraviolet Cured Ink Jet Prints. *Journal of Imaging Science and Technology*®. 54 (6), 060402-1-060402-9. Available from: doi: 10.2352/J.ImagingSci.Technol.2010.54.6.060402
- Feller, R. L. (1994) *Accelerated Aging: Photochemical and Thermal Aspects, Research in Conservation 4*. Marina del Rey, California, The Getty Conservation Institute, p. 280.
- Ha, Y.-B., Park, J.-Y. & Kim, H.-J. (2019) Influence of the Physical Properties of Digital Printing Paper on the Printing Quality. *Journal of Korea Technical Association of the Pulp and Paper Industry*. 51 (2), 108-120. Available from: doi: 10.7584/JKTAPPI.2019.04.51.2.108
- Izdebska, J., Żołek-Tryznowska, U. & Książek, T. (2013) Influence of artificial aging on cellulose film. The optical properties of printed and non-printed biodegradable film bases. *Agro FOOD Industry Hi Tech*. 24 (5), 52-56.
- Lind, J., Stack, J. & Everett, E. T. (2004) Fade Resistance of Lithographic Inks: A New Path Forward—Part 1. *GATFWorld*. 28-32.
- Małachowska, E., Przybysz, P., Dubowik, M., Kucner, M. & Buzala, K. (2015) Comparison of Papermaking Potential of Wood and Hemp Cellulose Pulps. *Ann. WULS - SGGW, Forestry and Wood Technology*. 91, 134-137.
- Miao, C., Hui, L.-F., Lui, Z. & Tang, X. (2014) Evaluation of Hemp Root Bast as a New Material for Papermaking. *Bioresources*. 9 (1), 132-142. Available from: doi: 10.15376/biores.9.1.132-142
- Narakornpijit, N. (2018) *A Study of the Lightfastness of High-Chroma Water-Based Flexographic Printing Inks*. PhD thesis. Rochester Institute of Technology.
- Plazonic, I., Barbaric-Mikocevic, Z. & Dzimbeg-Malcic, V. (2009) Office papers stability during accelerated ageing. In: Katalinic, B. (ed.) *DAAAM International Scientific Book 2009*. Vienna, Austria, DAAAM International, pp. 333-340.
- Plazonic, I., Barbaric-Mikocevic, Z. & Dzimbeg-Malcic, V. (2015) Optical stability of office papers treated with cocamidopropyl betaine. *Wood research*. 60 (2), 263-272.
- Plazonić, I., Barbarić-Mikočević, Ž., Bates, I. & Malnar, L. (2016) Chemical stability of prints made on hemp fibre based papers. *Acta Graphica*. 27 (3), 25-30.
- Plazonić, I., Bates, I., Džimbeg-Malčić, V. & Zember, D. (2020a) Colorimetric changes of waterbased flexographic ink printed on hemp-based papers exposed to artificial ageing. In: Dedijer, S. (ed.) *Proceedings - The Tenth International Symposium GRID 2020, GRID 2020, 12-14 November 2020, Novi Sad, Serbia*. Novi Sad, University of Novi Sad, Faculty of Technical Sciences, Department of Graphic Engineering and Design, pp. 57-62. Available from: doi: 10.24867/GRID-2020-p3
- Plazonic, I., Džimbeg-Malcic, V., Bates, I. & Barbaric-Mikocevic, Ž. (2020b) Effects of Photo-oxidation on the Properties of Hemp Office Papers, *International Journal of Technology*. 11 (2), 215-224. Available from: doi: 10.14716/ijtech.v11i2.3196
- Plazonić, I., Malnar, L., Džimbeg-Malčić, V., Barbarić-Mikočević, Ž. & Bates, I. (2018) Changes in the optical properties of hemp office papers due to accelerated ageing. In: Kašiković, N. (ed.) *Proceedings of 9th international symposium on graphic engineering and design, GRID 2018, 8-10 November 2018, Novi Sad, Serbia*. Novi Sad, University of Novi Sad – Faculty of Technical Sciences, Department of Graphic Engineering and Design, pp. 121-127. Available from: doi: 10.24867/GRID-2018-p14
- Radkova, V., Tsekova, P., Ivanova, T. & Valchev, I. (2015) Effect of dry-heat ageing on label paper quality. *Bulgarian Chemical Communications*. 47 (Specialissue A), 51-59.
- Zervos, S. (2010) Natural and Accelerated Ageing of Cellulose and Paper: A Literature Review. In: Lejeune, A., Deprez, T. (eds.) *Cellulose: Structure and Properties, Derivatives and Industrial Uses*. Hauppauge, New York, Nova Science Publishers Inc., pp. 155- 203.
- Żołek-Tryznowska, Z. & Annusik, T. (2019) Effect of various conditions of artificial ageing on selected properties of overprinted plastic films. *Inovacijos leidybos, poligrafijos ir multimedijos technologijose 2019*. 164-173.



© 2021 Authors. Published by the University of Novi Sad, Faculty of Technical Sciences, Department of Graphic Engineering and Design. This article is an open access article distributed under the terms and conditions of the Creative Commons Attribution license 3.0 Serbia (<http://creativecommons.org/licenses/by/3.0/rs/>).

Drying methods of the printing inks

ABSTRACT

Accelerating the transition to post-print processes needed in the printing industry and shortening the time the product's release time is closely related to the drying time of the ink film. The drying of fluid ink on the surface of the print substrate, transforming from liquid to solid occurs physically and chemically in several ways. Drying systems can be functional alone on the surface of the printing substrate for an ink film or depending on the chemical content of the ink and the properties of the printing substrate, drying can be achieved at the same time with more than one system. Recently, in order to reduce climate, environmental and health impacts and with the development of technology, significant changes are also being experienced in the printing industry and preferences are changing. In this study, more environmentally friendly LED UV and microwave drying systems that save time and energy together with existing basic drying systems such as absorption, evaporation, oxidation-polymerization and conventional UV used in the printing industry are examined. The advantages of different drying systems to the printing industry, preferred drying systems and new studies on this issue have been evaluated.

KEY WORDS


Drying system, UV-curing, LED-UV, microwave drying, radiation curing

Ashraf Abd El-Rahman

Elsayed Saad¹ 

Cem Aydemir² 

Samed Ayhan Özsoy³ 

Semiha Yenidoğan² 

¹Independent Consultant in Printing and Media Technology European and Arab Region, Wuppertal, Germany

²Marmara University, School of Applied Science, Department of Printing Technologies, Istanbul, Turkey

³Istanbul University- Cerrahpasa, Vocational School of Technical Sciences, Printing and Publication Technologies Program, Istanbul, Turkey

Corresponding author:

Cem Aydemir

e-mail:

cemaydemir@marmara.edu.tr

First received: 30.1.2021.

Revised: 19.3.2021.

Accepted: 24.3.2021.

Introduction

The visual quality of print results is substantially based on the optimal level of ink merging with a substrate, particularly the drying and stabilization process of ink on the substrate (Aydemir et al., 2019). Drying is when the ink changes from a liquid state to a solid state after it is transferred to the printing substrate

through the rollers and printing plate. The complete drying process required for the ink film is very important for finishing processes such as lacquering, coating, folding and cutting post-printing. (Aydemir, 2010).

In printing, the most important element is to obtain the correct substrate and ink combination (Aydemir & Yenidoğan, 2018). A physicochemical interaction

between paper and printing ink greatly determines the spreading of wet ink, as well as setting and drying (Aydemir, 2016). In the process of fluid ink settling and absorption onto the paper surface, the surface characteristics of the paper are extremely important. Depth and width differences on the paper surface can affect the quality parameters of the ink film, such as ink settling on the paper, print density, print gloss, and color (CIE L*a*b*) (Aydemir et al., 2021). Ink's structure and solvents are also determinants in the drying process of the ink. In addition, air, temperature, and humidity have a major influence on the drying speed of the ink.

With the increasing use of complex surfaces and inks, the need for different drying techniques has increased in the printing process. Sensitivity to environment and human health has also caused changes in drying systems (increasing use of water-based inks instead of solvent-based inks, etc.). Drying in the printing process generally takes place by the penetration or evaporation of the ink solvent into the printing substrate and the chemical change of the ink. A combination of two or more drying systems can be used to ensure final drying of the ink film. Some inks dry by a combination of two or more drying mechanisms, such as "penetration into the printing substrate" and "air oxidation" (McKinney, 1995; Brancher, 2019). For example, in the web-off-set heat-set drying process, some of the solvent oils evaporate from the ink, while some are absorbed by the printing substrate. The remaining part of the ink undergoes oxidation- polymerization and drying occurs.

Drying Methods of Printing Inks

Drying of the printed substrates is an important issue for the printing industry. The ink is expected to show good performance in terms of fluidity and adhesiveness during transfer from the ink fountain to the printing substrate during printing, and to dry after transfer to the printing substrate. Fast or slow drying creates difficulty in application. If the ink cannot penetrate fast enough into the paper, there can appear problems during the printing process of trapping issues, or, after the printing process, blocking, smearing, set-off to the back of the next sheet. If on the other hand the ink sets too fast, penetrates too fast into the paper, other problems can show up, like strike-through, trapping again and picking.

Drying of printing inks depends on the following factors:

- Printing method (offset, gravure, flexography etc.)
- Inks type (liquid, paste, water-based or organic solvent-based, radiation curing inks, etc.)
- Ink rheology (viscosity, flow, tack)
- Speed of printing machines
- Printing substrates (paper, foil, plastic etc.) and their properties

- The characteristics of the dryer systems (hot-air, cured systems, IR, etc.) (Saad, 2007).

The drying of the ink film is accomplished by physical (penetration, evaporation) processes and chemical reactions (oxidation or polymerization) or a combination of both, depending on the ink formulation and the properties of the printing substrate.

The main drying methods are as follows;

- Absorption drying
- Evaporation drying
- Oxidation and polymerization drying
- Radiation (Ultraviolet-Infrared-Microwave)

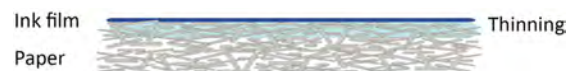
In general, gravure, flexography and web-off-set inks are by evaporation, sheet-fed offset inks are by oxidation-polymerization and cold-set inks are dried by absorption (Saad, 2007).

Absorption Drying

Printing inks consist mainly colorants (dyes or pigments), binders (natural resins, artificial resins, or plastics), solvent or solvent blend and additives. Drying by absorption occurs when the liquid components (predominantly solvent part) in the printed ink film are absorbed by the pores of the printing substrate. Absorption is an interaction between ink and printing substrate (Figure 1, 2). Generally, this type of drying method is depending on the carrier viscosity of the printing ink, the vehicle (binder) and the absorption capacity of the substrate (Saad, 2007). With absorption, drying occurs mainly on absorbent surfaces such as paper and cardboard, and several properties of these substrates manage the absorption of ink (Huber, 2013).



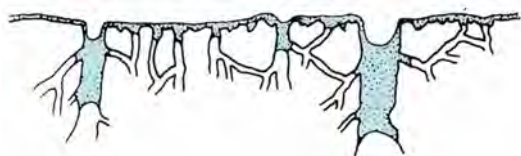
» **Figure 1:** Newly printed ink film on the top surface of the paper



» **Figure 2:** Absorbing ink film on the top surface of paper

The ink-absorption capacity is an important factor for evaluating the printing of paper (Dong, et al., 2020). The liquid absorption ability of paper and cardboard is based on micro capillarity (Imamoglu et al., 2013). In this drying technique, the printing substrate surface absorbs the solvent (solvent or mineral oil, etc.) in the wet ink film and separates it from the resin and pigment (Aydemir, Yenidoğan & Özsoy, 2020). Paper or cardboard acts as a filter with this feature (Aydemir &

Özakhun, 2014). Since the solvent is not fully compatible with the resin and pigment mixture in terms of its chemical structure, it dissociates and penetrates into the fine capillary fiber tubes of the paper horizontally and vertically at a very low speed (Figure 3) (Brancher, 2019). Thus, the released resin and pigment allow the formation of a hard and solid layer on the surface. A fully solidified ink film can sometimes be formed in 6 to 7 days. The absorption ability of the paper surface plays an important role in the drying of the ink (Brancher, 2019).



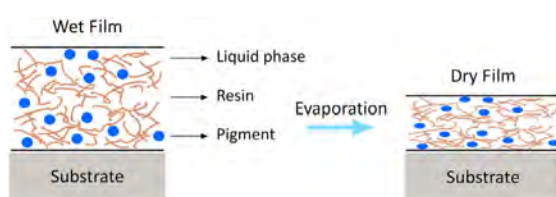
» **Figure 3:** Capillary structure of paper and absorption of ink

The pore structure of the paper is decisive for the absorption process of ink. If the pore diameter of the paper is small enough, only oil enters the paper, while the pigment and the rest of the vehicle remain on the surface. If the pore diameter of the paper is too large, the pigment and vehicle also penetrate the paper, which leads to a decrease in the color strength of the printed ink. Drying by means of absorption occurs faster and more intensively on its uncoated surfaces, while the absorption of ink on coated paper surfaces is quite slow and low in quantity.

Especially in cold-set offset printing, wet ink film dries by being absorbed by paper or penetrating into paper fiber body (Tsigonias et al., 2010). Absorption into the paper body also occurs in water-based and solvent-based inks. The viscosity of the ink is as effective as the pore structure of the paper in the absorption of the ink (Sunnerberg & Larsson, 1987).

Evaporation Drying

The fast evaporating solvents in the ink composition separate from the ink after printing and evaporate. The remaining binder combines with the pigment and creates a hard color layer on the printing surface. The evaporation of the liquid phase causes the remaining ink components to come into more contact with each other and create a continuous film (Figure 4) (Brancher, 2019).



» **Figure 4:** The appearance of pigment particles after evaporation of the ink

The reach of liquid ink to the desired density depends on the evaporation time of the solvent inside. As the liquid phase evaporates, the viscosity of the ink increases and the ink film begins to change from liquid to solid (Sappi Printer Technical Service, 2012). It then gives a dry ink film that adheres well to the print substrate (Brancher, 2019).

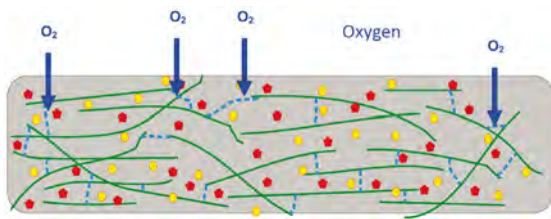
Solvents used in gravure, flexography and screen printing inks evaporate at room temperature. High temperature and heat energy are needed to remove the oil-based solvent used in heat-set offset printing inks (Aydemir, 1999). In the heat-set printing drying process, the paper is exposed to oven drier temperature of about 120-150°C so that the solvent (mineral oils in the boiling range of 85-120°C containing aliphatic hydrocarbons) in the printed ink film can evaporate (Aydemir, Akgül & Tutak, 2020; Smyth, 2003). The long hot-air dryer is used to blow hot-air over both sides of the fresh print via nozzles (Tsigonias et al., 2010). The local temperature rise in the dryer causes the ink solvent to evaporate.

Despite the above-mentioned facts, the evaporation drying method still has some problems:

- A longer time is required to dry water-based inks with evaporation methods. Because the drying of water-based inks is 4.5 times slower than solvent-based inks.
- Alcohol is used to improve the wetting and drying properties of water-based inks. Alcohol use (if there is an ammonia and amine group) causes environmental pollution.
- Most of the ink solvents that evaporate during the printing process are released into the atmosphere. Evaporating solvents are known to severely damage the ozone layer (Aydemir & Özsoy, 2020).
- During the evaporation of organic solvent-based inks, high capital investments are required in order to prevent the pollution caused by the waste air from the dryer exhaust in the atmosphere.
- Energy consumption is high.
- Drying systems for water-based and oil-based inks require considerable space to achieve complete drying.
- In flexography printing, excessive heat may cause the visco-elastic properties of plastic substrates to change.
- In heat-set web-offset printing, the possibility of overheating of the paper line can cause changes in the fiber size of the paper, with moisture loss in the non-printed areas of the paper substrate. Therefore, printing finishing processes are getting more and more difficult (Saad, 2007).
- With high heat, the printing substrate color and printing colors may change.

Oxidation and Polymerization Drying

This type of drying system depends on the chemical reaction between the oxygen in the atmosphere and the drying oil in the components of the carrier system (Saad, 2007). Except for the part (liquid phase) that is absorbed or evaporated after the ink is printed, the content that cannot enter the capillaries and remains on the paper surface (unsaturated vegetable oils such as linseed oil, soybean oil, tung oil, resins and pigments) polymerizes when exposed to atmospheric oxygen. (Figure 5) (Huber, 2013; PrintWiki, 2018). The oxygen in the air adds to double bonds of the drying oil molecules to form hydroperoxides (Saad, 2007). Thus, a rigid ink film with a thickness of 2- 3 micrometer is formed on the surface of the print substrate (Saad, 2007). In other words, the combination of the binding group molecules within the ink with the oxygen of the air enables the formation of new and larger molecules (molecular change). Also, since most molecules have more than one reactive site (i.e. double bonds), some cross-links form by forming a network (Saad, 2007) and the ink changes from a thin and soft state to a solid state. The drying of (sheet-fed) offset inks on the surface of less absorbent and non-absorbent printing papers usually occurs in this way.

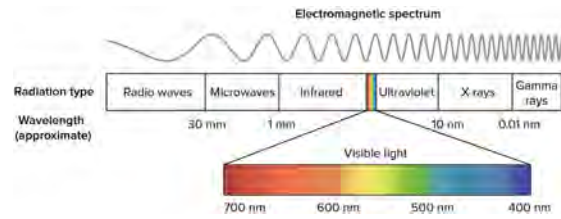


» **Figure 5:** Oxidative drying in offset printing

Following the physical drying process, the chemical drying time varies according to the oxygen uptake of the working environment and is accelerated by a heating (Smyth, 2003). Through initiators or catalysts (metal dryers such as cobalt, lead, manganese salt), oxygen in the air reacts more easily with the binding part of the ink and polymerization accelerates.

Radiation Drying

In cases where physical and chemical drying is insufficient, radiation and ink drying systems can be used. There are several types of radiation used to dry inks. These include ultraviolet radiation (UV), infrared (IR), microwave (MW) and radio frequency (RF). Each drying method determines the ink chemistry and the nature of the print ink used (Leach et al., 1988). Radiation drying types are preferred by printing enterprises because they increase the type of substrate and printing speed, accelerate the transition to post-printing processes, prevent drying problems of the ink, and reduce environmental effects (Figure 6).



» **Figure 6:** Radiation drying - Electromagnetic spectrum (Khan Akademy, 2017)

Ultraviolet (UV) Curing

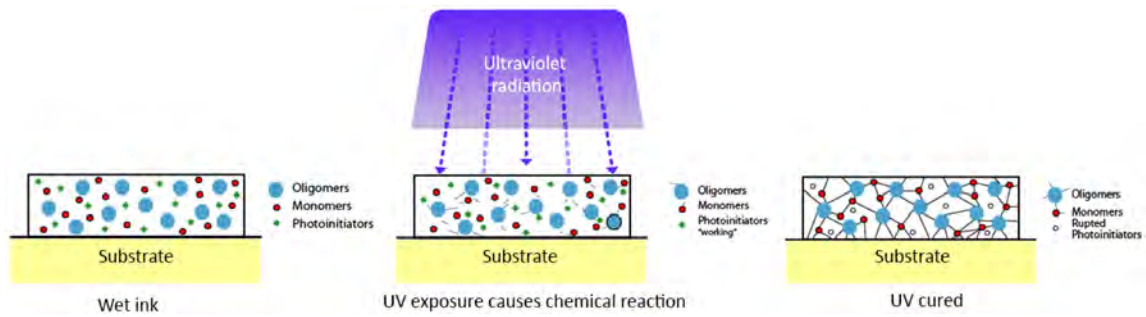
UV curing is a photo-polymerization process that uses UV energy source (the UV light) to transform a liquid into a solid. With the absorption of the UV energy, the photo-initiators contained in varnish, ink, adhesive or resin in the liquid state produce substances called free radicals, that react with the chemical compounds of the liquid substance, turning it into solid. This process is also called “polymerization” (PhotoElectronics, 2019; Kunwong, Sumanochitraporn & Kaewpirom, 2011). UV curing is widely used in sheet-fed offset printing, inkjet printing, screen printing and flexography printing where oxidation drying is insufficient, especially in packaging applications (Smyth, 2003; Leach et al., 1988).

For UV curing, UV-curable inks whose binder and solvent molecules react to UV radiation and form a fixed film layer in a short time must be used. These inks contain photo-initiators that absorb UV radiation and thus generate highly active chemical compounds known as free radicals (Argent, 2008).

UV inks is cured by a chemical polymerization reaction initiated by exposure to UV radiation and can therefore only be used in printing machines with UV curing systems (Aydemir, 1999; Brilliant Universal Limited, 2012). UV systems consist of beam source (lamp) and reflectors as in IR systems. UV dryers can be added to the output of printing machines or can be placed between printing units for intermediate drying (Argent, 2008).

UV curing uses light energy to initiate polymerization (Argent, 2008). Liquid ink is exposed to UV radiation by passing under the metal halide or mercury vapor arc lamps in the machine immediately after printing (Brancher, 2019). Strong UV radiation hits the photo-initiators in the ink and activates it, and the photo-initiators become macromolecules under the effect of the radiation. Liquid ink begins to harden. At the end of the reaction, cured or polymerized, a solid layer is formed that combines the pigment (Figure 7) (Smyth, 2003).

The curing speed of the ink; the spectral distribution of the lamp depends on the reactivity of the printing ink, the radiation and radiation distribution in the curing



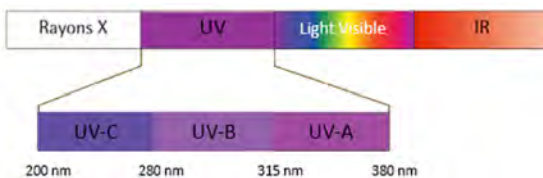
» **Figure 7:** *Ultraviolet curing*

plane, the thickness of the ink, the oxygen concentration (air or inert), the coating temperature conditions (Mehner, 1999).

Since different photo-initiators require different UV wavelengths, radiation from the source and photo-initiators must be matched to ensure polymerization (Hung, Wimberger & Mujumdar, 2006). For this purpose, UV lamps radiate light at different UV ranges to have maximum drying efficiency.

The UV radiation spectrum is located in a series of wavelengths shorter than visible light and can be divided into 3 parts:

- UV-C (200-280 nm) activates photo-initiators and lets the surface dry out.
- UV-B (280-315 nm) continues polymerization reaction.
- UV-A (315-380 nm) provides deep curing (Figure 8) (Brancher, 2019).



» **Figure 8:** *Ultraviolet wavelengths*

The power output and condition of lamps and reflectors significantly affect the amount of UV light energy the ink is exposed to (Argent, 2008).

Regardless of the type of dryer or ink used, it is very important to check the power rating, nature and condition of the lamps during printing, the printing speed and the compatibility of the amount of ink consumed.

If the inks do not dry adequately, several operations can be done, such as checking the efficiency and working hours of each lamp, and slowing down the printing speed (Brancher, 2019).

Advantages of the UV system:

1. The lack of solvent in UV ink makes UV curing an attractive alternative in situations where solvent emissions need to be reduced (Brilliant Universal Limited, 2012).
2. Print stability and print quality are very good in UV curing because the chemical reaction does not start during drying until energy is applied. Therefore, there is no volatile organic compounds (VOC) problem (Argent, 2008).
3. The UV curing process is very fast, usually completed within fractions of a second. This means less space required. Shelf or secondary drying processes are eliminated with UV curing (Brilliant Universal Limited, 2012).
4. Since the lamp reflectors in the dryer are cooled by air or water cooling equipment, the effect of the heat rays coming to the printing substrate decreases compared to the IR technique. This allows printing of certain heat-sensitive materials (PVC, polyester, etc.) of certain thickness.

LED-UV Curing

In the traditional UV curing process, quartz discharge lamps have been used for many years, and these lamps contain lead, mercury and cadmium metals (PhotoElectronics, 2019). The disadvantages of conventional UV systems are that they produce ozone, need exhaust systems to maintain air quality, use a lot of energy, and emit a lot of heat. Also, the disposal of used mercury arc vapor lamps is problematic. Because mercury is a toxic metal, it has attracted the attention of environmental regulators.

LED-UV are definitely the innovation of the future, offering many advantages in curing and drying industrial processes. For this reason, its use is increasing day by day. With the development of LED technology, changes are also experienced in UV curing systems. The LED-UV curing system uses diodes that convert electrical current into light. When the electrical current flows through an LED, it gives off IR or UV radiation. The UV light causes chemical reactions in the molecules within the liquid, forming chains of polymers until the liquid becomes a solid.

This process is a new technology that was designed to provide solutions to many of the issues found in conventional UV curing and heat-set drying (DoctorUV, 2018).

The LED-UV curing system, which is preferred in sheet-fed offset lithography and digital printing machines, allows printing on substrates with lower thickness and different heat-sensitive because it emits less heat than conventional UV systems. It also reduces electricity consumption and can contribute to a reduction in VOC (Mirković, Medek & Bolanča, 2019). LED-UV systems are more environmentally friendly due to odorless production, less heating and lower energy consumption. With these advantages, it provides an important alternative to conventional UV curing systems for solidifying inks, lacquers and adhesives (DoctorUV, 2018).

Infrared (IR) Drying

Infrared (IR) drying is a kind of radiant heating. In this drying system, no mechanical effects such as high-speed hot-air jets are required for heating. IR radiation may transfer large amounts of energy in short time. The energy emitted by IR radiation is directly used for heating the wet ink film (Saad, 2007). In this system, heat energy is generated when the ink film absorbs sufficient IR light energy. At high temperatures oxidation, penetration, evaporation and polymerization mechanisms all accelerate (Leach et al., 1988).

The wavelength spectrum of the radiation depends on the nature and temperature of the heat source. The wavelength range of thermal radiation is 0.75–1000 μm within the spectrum. IR radiation is conventionally classified as short-wave (0.75–3.00 μm), medium-wave (3.00–25 μm), and long-wave (25 μm – 1000 μm) (Figure 9), (Selim et al., 1997).

As the wavelength of the IR radiation is too long (much longer than the wavelength of UV radiation), the energy of their photons is too low (it is much lower than the energy of UV photons) to achieve any photochemical reactions. This means that, with IR radiation only a heating of the printed substrate is reached (Saad, 2007).

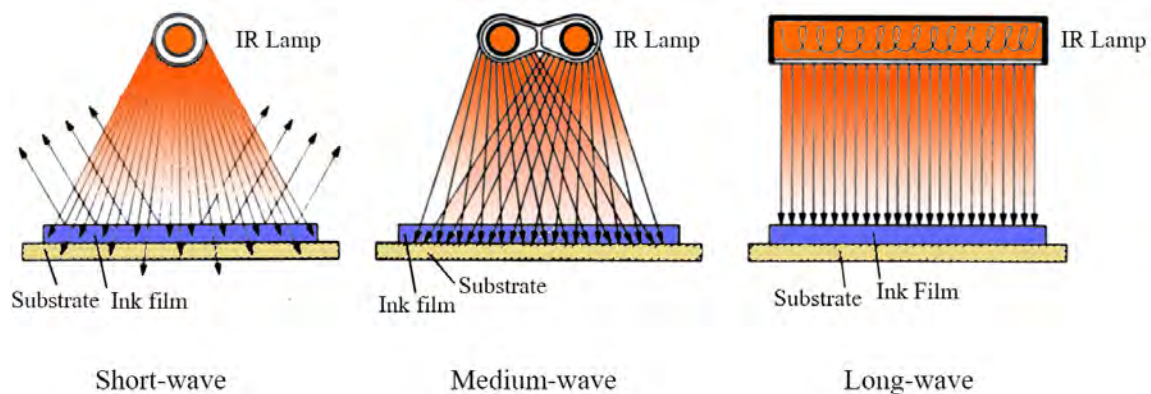
The most common current applications of IR drying in printing are dehydration of ink films (Ratti & Mujumdar, 2006). IR technology is mostly used to solve the drying problem of water-based inks, varnishes, lacquers and adhesives that cannot be evaporated. The spectrum of the medium wave radiator is very well matched to the absorption line of water, so it is highly efficient and economical in water-based ink drying (Jingxiang et al., 2019). Shortwave IR radiators, on the other hand, are effective in drying thick wet ink films due to their high penetrating power. Maximum drying sensitivity of offset printing inks is in the medium wavelength range of 3- 3.6 μm . It is important to adjust the IR wavelength for the absorption of the inks to substrates (Saad, 2007).

IR dryers are used in newspaper printing only to stimulate ink adsorption, thereby facilitating printing with higher ink density, that is, with higher ink application (Tsigonias et al., 2010). UV and IR drying systems can be used for drying inks as well as protective and decorative over-print varnish and lacquer applications.

Microwave (MW) Drying

Microwave (MW) drying is a technique based on electromagnetic waves that generate heat directly inside the ink film. MW radiation is a part of the electromagnetic spectrum ranging from 300 MHz to 300 GHz (Waghmare et al., 2021). This system effectively, quickly and efficiently dries the water-based inks on the paper.

Various liquid materials in printing such as inks, varnishes, lacquers, and adhesives contain high ratios of water. (Aydemir, Altay & Akyol, 2021). Water and other polar solvents are easily heated by microwave energy. Polar solvent molecules act like small magnet. The movement of molecules then generates heat. Under the action of the microwave electromagnetic field, the heated medium molecules become polarized molecules with positive and negative charges. Since the microwave field changes rapidly, solvent molecules oscillate and try to align with the field. MW are non-ionizing, they can interact with dielectric materials to generate heat by agitating molecules in an alternating electromag-



» **Figure 9:** Short, medium, long wavelength drying

netic field. While solvent-based inks are widely used in flexography, gravure and screen printing systems, the use of water-based inks is limited (Aydemir & Özsoy, 2020). Water-based inks create a drying problem due to the low evaporation rate of water (McKinney, 1995). Despite such problematic aspects of water-based inks, use to the instead of solvent-based inks is still greatly encouraged due to environmental and health concerns.

Infrared radiation or other hot-air drying methods, require a long drying period and large amounts of energy. Besides that, conventional drying mechanisms lead to, in certain cases, insufficient drying which results in misprints and added cost (Tsigonias et al., 2010). Using a microwave-assisted drying system has environmental benefits compared to a conventional drying system (Jingxiang et al., 2019). In addition, MW drying is known to provide extremely high energy savings compared to existing conventional drying technologies, although equipment costs are high (Sharma, 2015).

Marios et al. compared several drying methods common to water-based inks, hot-air drying, IR drying, MW drying speed and energy consumption (Tsigonias et al., 2010). The results proved that MW drying has distinct advantages in terms of both drying speed and energy consumption. In the study conducted by Marios, the energy consumption of MW drying was much less than that of hot-air drying.

Radio Frequency (RF) Drying

The principle of the RF drying method is very similar to MW drying. In this system, an alternating electric field is created between two electrodes. The material to be dried (for example glue, inks and paper, carton or others) is conveyed between the electrodes where the alternating electric field causes polar molecules in the material to continuously re-orient themselves to face opposite poles such like the way bar magnets behave in an alternating magnetic field. The friction resulting from molecular movement causes the material to rapidly heat throughout its entire printed ink film (Trembley & Loring, 1969).

Conclusion

It is important for ink manufacturers to test the placement behaviors of the ink and for paper manufacturers to control the absorption behaviors of the paper to improve the drying process. In this study, the drying methods used in the printing processes were evaluated in terms of printing substrate, ink and printing systems. According to this;

Drying systems can be functional alone on the surface of the printing material for an ink film, or multiple systems

can be active simultaneously, depending on the chemical content of the ink and the properties of the printing substrate. High-speed hot-air drying, IR drying, UV curing, MW drying and other conventional drying methods can be used together to increase the drying speed.

UV-curable inks and coatings contain low amounts of or no VOC. Therefore, UV curing systems can be preferred instead of evaporative drying systems using solvent-based inks. However, UV curing must be designed and used to meet all safety requirements of personnel and the environment due to biological effects on the skin and eyes and hazards from ozone, nitrogen oxide (NOx) and other by-products.

UV ink and UV over-print lacquers can cause large stains that cannot be easily removed with conventional de-inking methods and can be seen on recycled paper. This situation should not be overlooked in the selection of ink and drying system.

The MW drying method can be preferred in prints made with water-based ink and in cases where the printing substrate properties are not desired to be adversely affected. Because studies have shown that MW drying does not damage the ink-free areas of the paper. With a microwave-assisted drying system, both environmental benefits and energy and cost efficiency can be achieved compared to a conventional drying system.

Finally; Excessive ink consumption in the printing process will have negative effects on the economy and the environment due to higher consumption of resources to be used in drying energy. For this reason, the environmental sustainability of printing can be achieved by keeping ink consumption at an optimum level..

References

- Argent, D. (ed.) (2008) *Drying Part 3: Paste Inks*. Available from: <https://www.pffc-online.com/print/inks/6097-drying-part-paste-0401> [Accessed 20th February 2021].
- Aydemir, C. (1999) *Determination of the ideal drying temperature of heat-set web offset inks by vapor pressure method*. PhD thesis. Marmara University Institute of Natural and Applied Sciences.
- Aydemir, C. (2010) Time-dependent behavior of a sessile water droplet on various papers. *International Journal of Polymeric Materials*. 59 (6), 387-397. Available from: doi: 10.1080/00914030903538470
- Aydemir, C. & Özakhun, C. (2014) *Printing Materials Science*. Istanbul, Marmara University Publisher. pp. 262-264.
- Aydemir, C. (2016) A study on the printability properties of alkali-sized recycled papers. *Science and*

- Engineering of Composite Materials*. 23 (5), 565-571. Available from: doi: 10.1515/secm-2013-0266
- Aydemir, C. & Yenidođan, S. (2018) Light fastness of printing inks: A review. *Journal of Graphic Engineering and Design*, 9 (1), 37-43. Available from: doi: 10.24867/JGED-2018-1-037
- Aydemir, C., Karademir, A., Imamođlu, S., Altay, B. N., Fleming, P. D. & Tutak, D. (2019) Investigation of the evolution of hydrophobicity and wettability of paper in multi-color printing process. *Cellulose Chemistry and Technology*. 53 (7-8), 787-794. Available from: doi: 10.35812/CelluloseChemTechnol.2019.53.77
- Aydemir, C., Akgül, A. & Tutak, D. (2020) Effects of oven drying and polydimethylsiloxane (Pdms) emulsion coating on heat-set printing quality. *Cellulose Chemistry and Technology*. 54 (5-6), 495-503. Available from: doi: 10.35812/CelluloseChemTechnol.2020.54.50
- Aydemir, C., Yenidođan, S. & Özsoy, S. A. (2020) Effects of ink consumption on print quality on coated cellulose-based paper surfaces. *Cellulose Chemistry and Technology*. 54 (1-2), 89-94. Available from: doi: 10.35812/CelluloseChemTechnol.2020.54.10
- Aydemir, C. & Özsoy, S. A. (2020) Environmental impact of printing inks and printing process. *Journal of Graphic Engineering and Design*. 11 (2), 11-17. Available from: doi: 10.24867/JGED-2020-2-011
- Aydemir, C., Altay, B. N. & Akyol, M. (2021) Surface analysis of polymer films for wettability and ink adhesion. *Color Research & Application*. 46 (2), 488-499. Available from: doi:10.1002/col.22579
- Aydemir, C., Kašiković, N., Horvath, C. & Durdevic, S. (2021) Effect of paper surface properties on ink color change, print gloss and light fastness resistance. *Cellulose Chemistry and Technology*. 55 (1-2), 133-139. Available from: doi: 10.35812/CelluloseChemTechnol.2021.55.14
- Brancher (2019) *Drying*. Available from: <http://www.brancher.com/Drying.html?lang=en> [Accessed 15th September 2020].
- Brilliant Universal Limited (2012) *UV curing technology*. Available from: http://www.bul.com.hk/bul/en/technologies/uv_curing [Accessed 20th October 2020]
- DoctorUV (2018) *UV LED curing systems*. Available from: <https://www.doctoruv.com/uv-curing-systems/uv-led-curing> [Accessed 10th November 2020].
- Dong, Y., Wang, B., Ji, H., Zhu, W., Long, Z., & Dong, C. (2020) Effect of papermaking conditions on the ink absorption and overprint accuracy of paper. *BioResources*. 15 (1), 1397-1406. Available from: doi: 10.15376/biores.15.1.1397-1406
- Huber (2013) *Inkformation Brochure*. Available from: https://www.hubergroup.de/fileadmin/_migrated/content_uploads/INKFORMATION_4_en_02.pdf [Accessed 23rd October 2020].
- Hung, J. Y., Wimberger, R. J. & Mujumdar, A. S. (2006) Drying of coated webs. In: Mujumdar, A. S. (ed.) *Handbook of Industrial Drying*. 3rd Edition. Boca Raton, Florida, CRC Press, pp. 931-951.
- Imamoglu, S., Karademir, A., Pesman, E., Aydemir, C. & Atik C. (2013) Effects of flotation deinking on the removal of main colors of oil-based inks from uncoated and coated office papers. *BioResources*. 8 (1), 45-58. Available from: doi: 10.15376/biores.8.1.45-58
- Jingxiang, X., Jinyao, L., Haichao, L., Mingming, Z. & Jifei, C. (2019) Research progress on water-based ink drying technology. In: *IOP Conferans Series: Materials Science and Engineering*. 565: 012017, 9–11 May 2019, Sanya, China. Bristol, IOP Publishing. Available from: doi: 10.1088/1757-899X/565/1/012017
- Khan Academy (2017) *Electromagnetic spectrum*. Available from: <https://tr.khanacademy.org/science/biology/photosynthesis-in-plants/the-light-dependent-reactions-of-photosynthesis/a/light-and-photosynthetic-pigments> [Accessed 16th October 2020]
- Kunwong, D., Sumanochitraporn, N. & Kaewpirom, S. (2011) Curing behavior of a UV-curable coating based on urethane acrylate oligomer: the influence of reactive monomers. *Songklanakarin Journal of Science and Technology*. 33 (2), 201-207. Available from: <https://rdo.psu.ac.th/sjstweb/journal/33-2/0125-3395-33-2-201-207.pdf> [Accessed 9th February 2021]
- Leach, R. H., Armstrong, C., Brown, J. F., Mackenzie, M. J., Randall, L. & Smith H. G. (1988) *The Printing Ink Manual*. 4th ed., Dordrecht, Netherlands, Springer, Dordrecht. Available from: doi: 10.1007/978-94-011-7097-0
- McKinney, R. W. J. (1995) *Technology of Paper Recycling*. London, Blackie Academic & Professional.
- Mehnert, R. (1999) Excimer UV curing in printing. In: *7. International Conference on Radiation Curing, RADTECH ASIA'99, 24-26 August 1999, Kuala Lumpur, Malaysia*. pp. 75-89. Available from: https://inis.iaea.org/collection/NCLCollectionStore/_Public/31/016/31016304.pdf [Accessed 25th January 2021]
- Mirković, I. B., Medek, G. & Bolanča, Z. (2019) Ecologically sustainable printing: Aspects of printing materials. *Technical Gazette*. 26 (3), 662-667. Available from: doi: 10.17559/TV-20180620181128
- PhotoElectronics (2019) *Benefits of UV LED curing lamps*. Available from: <https://www.photoelcuring.com/en/technologies/uv-led/benefits-led-uv-curing-lamps/> [Accessed 20th August 2020]
- PrintWiki (2018) *Oxidation*. Available from: <http://printwiki.org/Oxidation> [Accessed 5th November 2019]
- Ratti, C. & Mujumdar, A. S. (2006) Infrared drying. In: Mujumdar, In: Mujumdar, A. S. (ed.) *Handbook of Industrial Drying*. 3rd Edition. Boca Raton, Florida, CRC Press, pp. 423-438.
- Saad, A. A. E. R. E. (2007) *Environmental pollution reduction by using VOC-free water-based gravure inks and drying them with a new drying system based on dielectric heating*. PhD thesis. Bergische Universität Wuppertal.
- Sappi Printer Technical Service (2012) *Slow ink set & dry*. Available from: <https://cdn-s3.sappi.com/>

- s3fs-public/sappietc/Slow%20Ink%20Set%20and%20Dry.pdf [Accessed 30th November 2020]
- Selim, M. S., Yesavage, V. F., Chebbi, R., Sung, S. H., Borch, J. & Olson, J. M. (1997) Drying of water-based inks on plain paper. *Journal of Imaging Science and Technology*. 41 (2), 152-158. Available from: <https://www.ingentaconnect.com/contentone/ist/jist/1997/00000041/00000002/art00009> [Accessed 23rd December 2020]
- Sharma, S. K. (2015) Paper drying by using microwaves as heating source, Apex Institute of Engineering and Technology, Jaipur, Rajasthan India. Available from: https://www.academia.edu/12390349/Paper_Drying_By_Using_Microwaves_As_Heating_Source [Accessed 28th November 2020]
- Sunnerberg, G. & Larsson, L. O. (ed.) (1987) *Paper structure and its influence upon paper-ink interaction. Topical themes in newsprint - printing research*. Sweden, Swedish Newsprint Research Centre (TFL).
- Smyth, S. (2003) *The Print and Production Manual, Printing Inks*. 9th ed. Leatherhead, United Kingdom, Pira International Ltd.
- Trembley, J. F. & Loring C. M. (1969) Drying printing inks and coatings by radio frequency heating. *TAPPI*, 52 (10): 1847.
- Tsigonias, M., Ploumi, E., Politis, A. & Vekinis, G. (2010) Using microwave drying systems in the graphic arts, Modern solutions for environmental industrial applications. In: Enlund, N. and Lovreček, M. (eds.) *37th International Research Conference of Iarigai, Advances in Printing and Media Technology. September, Montreal, Canada*. Darmstadt, International Association of Research Organizations for the Information, Media and Graphic Arts Industries. pp. 291-296. Available from: [http://jpmtr.org/Advances-Vol-37\(2010\)_online.pdf](http://jpmtr.org/Advances-Vol-37(2010)_online.pdf) [Accessed 29th December 2020].
- Waghmare, R. B., Perumal, A. B., Moses, J. A. & Anandharamakrishnan, C. (2021) Recent developments in freeze drying of foods. In: *Innovative Food Processing Technologies, A Comprehensive Review*. Amsterdam, Netherlands, Elsevier, pp. 82-99. Available from: doi: 10.1016/B978-0-12-815781-7.00017-2



© 2021 Authors. Published by the University of Novi Sad, Faculty of Technical Sciences, Department of Graphic Engineering and Design. This article is an open access article distributed under the terms and conditions of the Creative Commons Attribution license 3.0 Serbia (<http://creativecommons.org/licenses/by/3.0/rs/>).



Impact of packaging shape and material on consumer expectations

ABSTRACT

Packaging appearance is important in evoking consumer impressions. No study has yet explored how two prominent packaging attributes, shape and material, affect the consumers' impressions and their expectations in the case of coffee products. Therefore, the objective of this study was to investigate whether the packaging shape has an impact on the taste intensity expected by the consumer, and whether packaging materials influence the expected coffee quality. In an online experiment, 115 participants evaluated different packaging samples. They rated the expected taste intensity for packaging samples that varied in shape complexity (i.e., cylindrical, rounded-angular, hexagonal and multifaceted). They also rated the expected coffee quality for packaging samples that varied in material (i.e., plastic, aluminium, glass and metal). The results showed that the packaging with a higher degree of shape complexity was associated with a higher taste intensity. Furthermore, we found a negative effect of glass on the expectation of product quality. The findings could be applied in product packaging design which aims to match the expected and actual characteristics of the product.

KEY WORDS

Packaging, coffee, shape, material, expected taste, perceived quality

Suzana Poslon
Dorotea Kovačević 
Maja Brozović 

University of Zagreb,
Faculty of Graphic Arts,
Zagreb, Croatia

Corresponding author:
Dorotea Kovačević
e-mail: dorotea.kovacevic@grf.hr

First received: 8.2.2021.

Revised: 23.4.2021.

Accepted: 5.5.2021.

Introduction

Packaging appearance is important because it is the only form of communication between the product and the buyer during the first purchase (Dadras, 2015). A well-designed combination of packaging attributes with certain visual elements can evoke emotional reactions from the consumers. The most prominent packaging attributes, which contribute to the packaging appearance at first glance, are shape and material.

Previous studies showed that consumers are sensitive to visual shapes on the packaging. For example, a study by Westerman et al (2013) demonstrated a greater tendency towards designs which use round elements on packaging labels in the case of vodka and water. According to Hassan, Lee & Peng (2012), the packaging shape is one of the two attributes that influences a purchase decision the most. The shape of packaging varies according to purpose and product type. Sometimes, deviation

of packaging form from existing packaging design in a product category may draw more attention from the consumers (Schoormans & Robben, 1997). Packaging shape can make the product more attractive and help consumers predict the volume of the product and its monetary value. In the area of food products, it can also impact the perception of product taste. The taste sensation (i.e., sweet, salty, bitter, acidic) can be activated even without consuming the product. This is commonly done through the visual design of the packaging, such as pictorial content and colours, but it can also be achieved through packaging shape (Velasco et al., 2014). If the shape corresponds to the actual taste of the product, the compatibility effect is perceived through two modalities: vision and taste, resulting in consumer satisfaction. If the consumers' created sensory and hedonic expectations do not match the actual taste of the product, there is a greater possibility for the consumers' dissatisfaction with the product and a decreased likelihood of repurchase (Ares & Deliza, 2010).

Another attribute that significantly influences the consumers' perception of the packaging is the material. Several studies from the last decade demonstrated the impact of the material on the participants' reactions. Kobayashi & Benassi (2015) reported on the importance of the shape of glass jars for the consumers' acceptance and purchase intention. Steenis et al. (2017) found that the packaging material affects the perception of sustainability, but also the perception of taste and quality. Labbe Pineau & Martin (2013) revealed that the visual, auditory and tactile sensory diversity of the packaging materials result in differences in the consumers' expectations. Ferreira (2019) manipulated both the texture of the packaging material as well as the product texture and demonstrated their impact on taste perception.

Altogether, previous packaging-oriented researches suggest that both the shape and the material can influence people's perception and their responses to packaging. Thus, the focus of our study was on these packaging characteristics and their impact on the consumers' expectations from the product.

Problem statement

The investigation of the association between shapes and different flavours was interesting to researchers (Turoman et al., 2018). The existing literature suggests that packaging shape can be one of the influential factors in forming peoples' impressions about product taste. Previous studies (Velasco et al., 2014; Velasco et al., 2016) confirm that there is a connection between the shape and the taste. They found a correlation between sweet taste and rounded forms. On the other hand, sour and bitter flavours were more correlated with angular and sharp forms. Spence & Ngo (2012) reported on the connection between stringent forms and an increase of bitterness, as well as the association of dairy and mint tastes with rounded shapes. Rounded shapes were also investigated in the study by Wang et al (2017) which showed that a round-shaped product is expected to be sweeter and less bitter than an angular-shaped one.

While most of the previous research was focused on sweet food products, our study went further in the examination of taste expectations in relation to packaging shape, by focusing specifically on coffee taste. Although there was a significant research interest in this popular drink (Harith, Ting & Zakaria, 2014; Van Loo et al., 2015; van Ooijen et al., 2017; Wever et al., 2010), none of the previous studies reported on the possible connections between the expected coffee taste intensity and the shape of its packaging. So, our first hypothesis was:

H₁: Packaging shape has an influence on the expected taste intensity of the coffee.

Besides the packaging shape, its material can also affect people's perception of the product (Ferreira, 2019; Kobayashi & Benassi, 2015), especially its perceived quality (Steenis et al., 2017). Consumers' expectations about the product quality can be based on various aspects of the material, such as sustainability (Steenis et al., 2017; Vukoje et al., 2020), texture (Ferreira, 2019), transparency (Chandran, Batra & Lawrence, 2009; Sabo et al., 2017) and coating (Cigula et al., 2020; Dolić, Pibernik & Majnarić, 2014; Hudika et al., 2020; Pibernik et al., 2020). From a practical viewpoint, all of these aspects mostly arise from product type, its specifications and requirements for its protection. When it comes to coffee products, their expected quality was investigated in the area of ready-to-drink beverages (Wang & Yu, 2016) and product packaging design (van Ooijen et al., 2017). However, consumers' expectations about coffee quality have not been examined in relation to variations of packaging material. Accordingly, our second hypothesis was:

H₂: Packaging material has an influence on the expected quality of the coffee.

Methodology

In order to test the hypotheses, we conducted an online survey which consisted of two main parts. The first part of the survey included four samples of the packaging that varied according to shape, from cylindrical to multifaceted. For the second part of the survey, we used four different samples of the packaging which varied according to material.

The survey was active from 28.4.2020. to 9.5.2020. It included 115 respondents and all of them were over 18 years old. Only those who claimed that they consume coffee at least once a month were included. The highest percentage of participants ranged from 18 to 50 years of age (95.7%), while only 5 participants (4.3%) were older than 50. 57.2% were women and 42.8% were men. 51.3% of participants claimed that they drink coffee several times a day, 28.7% drink coffee once a day, 15,4% drink coffee several times a week and 4,6% drink coffee several times a month.

In line with previous studies which dealt with food packaging (Ares & Deliza, 2010; Velasco et al., 2014), images of empty coffee packaging were used in our study. For the first part of the survey, the images of different glass coffee containers were presented to the participants. Figure 1 shows the containers. Their packaging shape varied in complexity, and they were classified into four main packaging shapes; cylindrical (A), rounded-angular (B), hexagonal (C) and multifaceted packaging (D). The packaging volume was 250 g, all of them were transparent, with the same lid colour and on the same background. The participants were asked to rate the expected coffee

taste intensity for each packaging shape. The ratings were recorded using a five-point Likert scale ranging from 1 (low intensity) to 5 (high intensity).

In the second part of the survey, we used images of different packaging that varied in materials, which resulted in four different packaging samples shown in Figure 2; a plastic bag (E), aluminium packaging (F), a glass container (G) and a metal box (H). All packaging samples were in a neutral colour and had the same volume of 250 g. The participants were asked to rate the expected coffee quality for each packaging sample, using a five-point Likert scale ranging from 1 (low quality) to 5 (high quality).



» **Figure 1:** Packaging samples used for the expected taste intensity

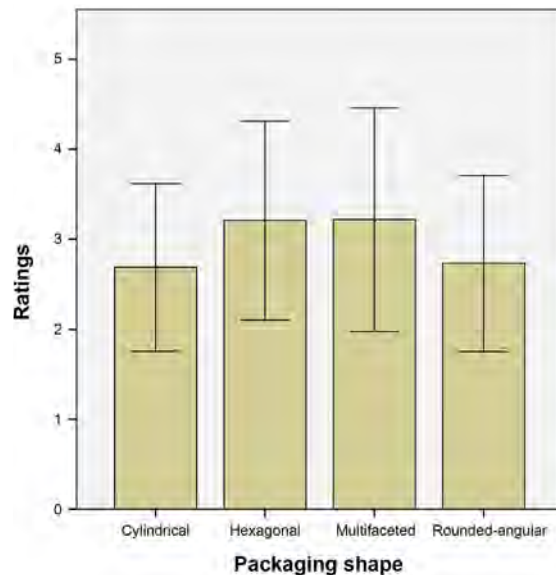


» **Figure 2:** Packaging samples used for the expected coffee quality

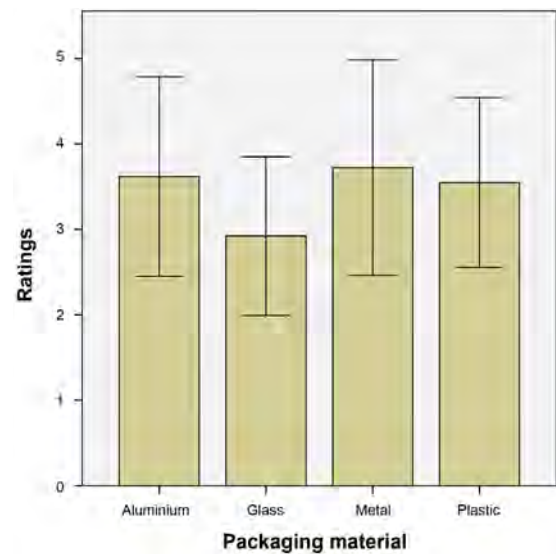
Results

In order to test our hypotheses, a repeated measures ANOVA was used. There was a significant effect of the packaging shape on the expected taste intensity, $F(3,342) = 12.30$, $p < 0.05$. Post hoc tests were conducted with the Bonferroni correction (adjusted level of significance was set at $p < 0.008$). The results showed that the participants expected the same taste intensity of the coffee in the cylindrical and rounded-angular packaging, $p > 0.008$. They also expected the same taste intensity of the coffee in the hexagonal and multifaceted packaging, $p > 0.008$. However, the cylindrical packaging was associated with lower taste intensity ratings ($M = 2.69$, $SD = 0.93$) than the hexagonal packaging ($M = 3.21$, $SD = 1.10$), $p < 0.008$, and the multifaceted packaging ($M = 3.22$, $SD = 1.24$), $p < 0.008$. Furthermore, the rounded-angular packaging was also associated with lower taste intensity ratings ($M = 2.73$, $SD = 0.98$) than the hexagonal packaging ($p < 0.008$), and the multifaceted packaging, $p < 0.008$. Figure 3 illustrates these results.

For the expected quality (see Fig. 4), the analysis showed that the packaging material affects the participants' expectations of the coffee quality $F(3,342) = 13.52$, $p < 0.05$. Post hoc tests were conducted with the Bonferroni correction and an adjusted level of significance ($p < 0.008$). There were no statistical differences in the expected quality between the coffee in the plastic bag, aluminium packaging and the metal box, all $p > 0.008$. However, the quality was perceived as significantly lower for the glass container ($M = 2.92$, $SD = 0.93$) than for the plastic bag ($M = 3.55$, $SD = 0.99$, $p < 0.008$), aluminium packaging ($M = 3.62$, $SD = 1.17$, $p < 0.008$) and the metal box ($M = 3.72$, $SD = 1.26$, $p < 0.008$).



» **Figure 3:** Mean ratings and standard deviation for the expected taste intensity



» **Figure 4:** Mean ratings and standard deviation for the expected quality

Discussion

The results of our study confirmed both of our hypotheses. In particular, the packaging shape had an impact on the participants' ratings of the expected taste intensity, and the packaging material influenced their ratings of the expected coffee quality.

Becker et al (2011) have reported on the impact of packaging shape on the expected flavour in the case of yoghurt, and Heuvelmans's research (Heuvelmans, 2017) confirmed this in the case of chocolate. The results of our study confirmed it in the case of coffee as well. The participants perceived the cylindrical and the rounded-angular packaging as coffee with a lower taste intensity. However, the participants expected that more complex packaging shapes (i.e., the hexagonal and the multifaceted packaging) contained coffee with a high taste intensity. The connection between the angular shaped packaging and higher taste intensity is not surprising. Previous research showed that angular forms can affect the taste intensity in the case of yoghurt (Becker et al., 2011). Furthermore, Velasco et al (2016) confirmed that there is a correlation between bitter taste, which is the main flavour of coffee, and sharp forms. Similar results can also be found in recent research focused on coffee. Sousa, Carvalho & Pereira (2020) investigated people's expectations of coffee acidity and sweetness in different packaging design conditions. They found that angular graphic elements printed on the packaging increased the expectations of acidity more than rounded elements. By connecting their results with those in our study, it is not unreasonable to expect that the combination of angular packaging with angular graphic elements printed on it may result in the consumers' predictive expectations of the coffee taste. However, this area should definitely be more investigated to provide research-based evidence for this valuable design guideline.

When it comes to packaging material, our study demonstrated the negative effect of glass containers on the expected quality, since the glass container was rated significantly lower than the plastic bag, aluminium packaging and the metal box. Among all packaging samples in our study, the glass container was the only packaging made of a transparent material which enables light penetration. It is known that light can affect food and beverage quality (Duncan & Hannah, 2012) and cause oxidation (Pristouri, Badeka & Kontominas, 2010). Thus, it is likely that the participants associated the packaging material's light transmission with a decreased level of coffee aroma and quality. A study by Kobayashi and Benassi (2015) revealed similar results. The participants in their experiment were not keen on selecting glass coffee packaging unless it used modern forms that enable better visualization of the actual product. Our results confirm other previously reported scientific conclusions on consumer expectations of coffee quality.

For example, Harith et al (2014) reported that packaging can stimulate the perception of coffee quality. Fenko, de Vries & van Rompay (2018) showed that packaging can guide the evaluation of the coffee product. Wang & Yu (2016) demonstrated that packaging appearance can play a critical role in generating consumer perception of the product value. All these findings suggest that packaging design should not be underestimated in the process of transmitting the message about the product quality. The impact of different environmental aspects of people's experiences of drinking coffee should also be taken into consideration in this process (Spence & Carvalho, 2020).

Conclusions

This study explored people's expectations of coffee in relation to its packaging attributes. The results revealed a significant effect of packaging shape on the expected taste intensity and the impact of packaging material on the consumers' perception of the coffee quality. The findings could be applied to future packaging design for certain types of coffee. Strong taste can be presented by increasing the level of packaging shape complexity. For example, cylindrical packaging can be used for mild coffee, while multifaceted packaging can be used for strong coffee. Consumers' expectations of low coffee quality can be avoided by using non-transparent packaging materials, such as metal box. Matching the expected and actual characteristics of the coffee product may create better trust between the consumer and the producer, which opens up possibilities for greater consumer satisfaction.

Since the online survey was conducted using two-dimensional photographs as stimuli, the study's main limitation is no physical contact between the participants and the realistic three-dimensional packaging samples. Viewing the samples in their actual structural form may, perhaps, evoke more noticeable effects on the participants' impressions and, consequently, their subjective expectations. Undoubtedly, despite the great scientific interest in packaging design, this area is still undeveloped and needs further research. Introducing a greater number of packaging variations for each material group could also provide useful insights. Future studies should also include coffee tasting tests which would provide wider research-based knowledge on the packaging's effects on the perception of taste in a realistic context.

References

- Ares, G. & Deliza, R. (2010) Studying the influence of package shape and colour on consumer expectations of milk desserts using word association and conjoint analysis. *Food Quality and Preference*. 21 (8), 930–937. Available from: doi: 10.1016/j.foodqual.2010.03.006

- Becker, L., van Rompay, T. J. L., Schifferstein, H. N. J. & Galetzka, M. (2011) Tough package, strong taste: The influence of packaging design on taste impressions and product evaluations. *Food Quality and Preference*. 22 (1), 17–23. Available from: doi: 10.1016/j.foodqual.2010.06.007
- Chandran, S., Batra, R. K. & Lawrence, B. (2009) Is seeing believing? Consumer responses to opacity of product packaging. *NA - Advances in Consumer Research*. 36.
- Cigula, T., Hudika, T., Katana, M., Golik Krizmanić, M. & Tomašegović, T. (2020) The influence of PCL-ZnO coating composition on coated offset cardboard prints. In: Dedijer, S. (Ed.), *Proceedings - The Tenth International Symposium GRID 2020, 12-14 November 2020, Novi Sad, Serbia*. Novi Sad, Faculty of Technical Sciences, pp. 101–108. Available from: doi: 10.24867/grid-2020-p8
- Dadras, A. (2015) Impact of shapes in packaging design on consumer behaviour in the lens of Kano's attractive quality theory. *International Journal of Scientific Research and Management Studies*. 2 (1), 78–86.
- Dolić, J., Pibernik, J. & Majnarić, I. (2014) Influence of UV varnish pattern effect on print quality. *Journal of Imaging Science and Technology*. 58 (6), 1–9. Available from: doi: 10.2352/J. ImagingSci.Technol.2014.58.6.060501
- Duncan, S. E. & Hannah, S. (2012) Light-protective packaging materials for foods and beverages. In: Kit, L. Y. & Dong, S. L. (eds.) *Emerging Food Packaging Technologies*. Cambridge, United Kingdom, Woodhead Publishing, pp. 303–322. Available from: doi: 10.1533/9780857095664.3.303
- Fenko, A., de Vries, R. & van Rompay, T. (2018) How strong is your coffee? The influence of visual metaphors and textual claims on consumers' flavor perception and product evaluation. *Frontiers in Psychology*. 9, 1–12. Available from: doi: 10.3389/fpsyg.2018.00053
- Ferreira, B. M. (2019) Packaging texture influences product taste and consumer satisfaction. *Journal of Sensory Studies*. 34 (6), 1–9. Available from: doi: 10.1111/joss.12532
- Harith, Z. T., Ting, C. H. & Zakaria, N. N. A. (2014) Coffee packaging: Consumer perception on appearance, branding and pricing. *International Food Research Journal*. 21 (3), 849–853.
- Hassan, S. H., Lee, W. L. & Peng, W. W. (2012) The influence of food product packaging attributes in purchase decision: A study among consumers in Penang, Malaysia. *Journal of Agribusiness Marketing*. 5, 14–28.
- Heuvelmans, A. (2017) *The influence of packaging shape on perceived taste for familiar and unfamiliar brands*. MSc thesis. Faculteit der Letteren
- Hudika, T., Tomašegović, T., Cigula, T. & Prša, M. (2020) Polycaprolactone primers with zinc oxide and silicon dioxide nanoparticles for paper substrates: Influence on the properties of cyan and magenta offset prints. *Coloration Technology*. 136 (5), 435–449. Available from: doi: 10.1111/cote.12487
- Kobayashi, M. L. & Benassi, M. de T. (2015) Impact of packaging characteristics on consumer purchase intention: Instant coffee in refill packs and glass jars. *Journal of Sensory Studies*. 30 (3), 169–180. Available from: doi: 10.1111/joss.12142
- Labbe, D., Pineau, N. & Martin, N. (2013) Food expected naturalness: Impact of visual, tactile and auditory packaging material properties and role of perceptual interactions. *Food Quality and Preference*. 27 (2), 170–178. Available from: doi: 10.1016/j.foodqual.2012.06.009
- Pibernik, J., Tomašegović, T., Mahović Poljaček, S. & Madžar, A. (2020) Consumer's experience of tea packaging as environment-friendly. In: Dedijer, S. (Ed.), *Proceedings - The Tenth International Symposium GRID 2020, 12-14 November 2020, Novi Sad, Serbia*. Novi Sad, Faculty of Technical Sciences, pp. 317–325. Available from: doi: 10.24867/grid-2020-p35
- Pristouri, G., Badeka, A. & Kontominas, M. G. (2010) Effect of packaging material headspace, oxygen and light transmission, temperature and storage time on quality characteristics of extra virgin olive oil. *Food Control*. 21 (4), 412–418. Available from: doi: 10.1016/j.foodcont.2009.06.019
- Sabo, B., Bečica, T., Keleš, N., Kovačević, D. & Brozović, M. (2017) The impact of packaging transparency on product attractiveness. *Journal of Graphic Engineering and Design*. 8 (2), 5–9. Available from: doi: 10.24867/JGED-2017-2-005
- Schoormans, J. P. L. & Robben, H. S. J. (1997) The effect of new package design on product attention, categorization and evaluation. *Journal of Economic Psychology*. 18 (2–3), 271–287. Available from: doi: 10.1016/S0167-4870(97)00008-1
- Sousa, M. M. M. D., Carvalho, F. M. & Pereira, R. G. F. A. (2020) Colour and shape of design elements of the packaging labels influence consumer expectations and hedonic judgments of specialty coffee. *Food Quality and Preference*. 83, 103902. Available from: doi: 10.1016/j.foodqual.2020.103902
- Spence, C. & Carvalho, F. M. (2020) The coffee drinking experience: Product extrinsic (atmospheric) influences on taste and choice. *Food Quality and Preference*. 80, 103802. Available from: doi: 10.1016/j.foodqual.2019.103802
- Spence, C. & Ngo, M. K. (2012) Assessing the shape symbolism of the taste, flavour, and texture of foods and beverages. *Flavour*. 1 (1), 1–13. Available from: doi: 10.1186/2044-7248-1-12
- Steenis, N. D., van Herpen, E., van der Lans, I. A., Ligthart, T. N. & van Trijp, H. C. M. (2017) Consumer response to packaging design: The role of packaging materials and graphics in sustainability perceptions and product evaluations. *Journal of Cleaner Production*. 162, 286–298. Available from: doi: 10.1016/j.jclepro.2017.06.036

- Turoman, N., Velasco, C., Chen, Y. C., Huang, P. C. & Spence, C. (2018) Symmetry and its role in the crossmodal correspondence between shape and taste. *Attention, Perception, and Psychophysics*. 80 (3), 738–751. Available from: doi: 10.3758/s13414-017-1463-x
- Van Loo, E. J., Caputo, V., Nayga, R. M., Seo, H. S., Zhang, B. & Verbeke, W. (2015) Sustainability labels on coffee: Consumer preferences, willingness-to-pay and visual attention to attributes. *Ecological Economics*. 118, 215–225. Available from: doi: 10.1016/j.ecolecon.2015.07.011
- van Ooijen, I., Fransen, M. L., Verlegh, P. W. J. & Smit, E. G. (2017) Packaging design as an implicit communicator: Effects on product quality inferences in the presence of explicit quality cues. *Food Quality and Preference*. 62, 71–79. Available from: doi: 10.1016/j.foodqual.2017.06.007
- Velasco, C., Salgado-Montejo, A., Marmolejo-Ramos, F. & Spence, C. (2014) Predictive packaging design: Tasting shapes, typefaces, names, and sounds. *Food Quality and Preference*. 34, 88–95. Available from: doi: 10.1016/j.foodqual.2013.12.005
- Velasco, C., Woods, A. T., Petit, O., Cheok, A. D. & Spence, C. (2016) Crossmodal correspondences between taste and shape, and their implications for product packaging: A review. *Food Quality and Preference*. 52, 17–26. Available from: doi: 10.1016/j.foodqual.2016.03.005
- Vukoje, M., Bolanča Mirković, I., Bešlić, M. & Petković, G. (2020) The influence of artificial aging on recyclability and mechanical stability of pharmaceutical packaging. In: Dedijer, S. (Ed.), *Proceedings - The Tenth International Symposium GRID 2020, 12-14 November 2020, Novi Sad, Serbia*. Novi Sad, Faculty of Technical Sciences, pp. 251–259. Available from: doi: 10.24867/GRID-2020-p27
- Wang, E. S. T. & Yu, J. R. (2016) Effect of product attribute beliefs of ready-to-drink coffee beverages on consumer-perceived value and repurchase intention. *British Food Journal*. 118 (12), 2963–2980. Available from: doi: 10.1108/BFJ-03-2016-0128
- Wang, Q. J., Reinoso Carvalho, F., Persoone, D. & Spence, C. (2017) Assessing the effect of shape on the evaluation of expected and actual chocolate flavour. *Flavour*. 6 (2), 1–6. Available from: doi: 10.1186/s13411-017-0052-1
- Westerman, S. J., Sutherland, E. J., Gardner, P. H., Baig, N., Critchley, C., Hickey, C., Mehigan, S., Solway, A. & Zervos, Z. (2013) The design of consumer packaging: Effects of manipulations of shape, orientation, and alignment of graphical forms on consumers' assessments. *Food Quality and Preference*. 27 (1), 8–17. Available from: doi: 10.1016/j.foodqual.2012.05.007
- Wever, R., van Onselen, L., Silvester, S. & Boks, C. (2010) Influence of packaging design on littering and waste behaviour. *Packaging Technology and Science*. 23 (5), 239–252. Available from: doi: 10.1002/pts.892



